

Molecular features of triple negative breast cancer cells by genome-wide gene expression profiling analysis

MASATO KOMATSU^{1,2*}, TETSURO YOSHIMARU^{1*}, TAISUKE MATSUO¹, KAZUMA KIYOTANI¹, YASUO MIYOSHI³, TOSHIHITO TANAHASHI⁴, KAZUHITO ROKUTAN⁴, RUI YAMAGUCHI⁵, AYUMU SAITO⁶, SEIYA IMOTO⁶, SATORU MIYANO⁶, YUSUKE NAKAMURA⁷, MITSUNORI SASA⁸, MITSUO SHIMADA² and TOYOMASA KATAGIRI¹

¹Division of Genome Medicine, Institute for Genome Research, The University of Tokushima; ²Department of Digestive and Transplantation Surgery, The University of Tokushima Graduate School; ³Department of Surgery, Division of Breast and Endocrine Surgery, Hyogo College of Medicine, Hyogo 663-8501; ⁴Department of Stress Science, Institute of Health Biosciences, The University of Tokushima Graduate School, Tokushima 770-8503; Laboratories of ⁵Sequence Analysis, ⁶DNA Information Analysis and ⁷Molecular Medicine, Human Genome Center, Institute of Medical Science, The University of Tokyo, Tokyo 108-8639; ⁸Tokushima Breast Care Clinic, Tokushima 770-0052, Japan

Received September 22, 2012; Accepted November 6, 2012

DOI: 10.3892/ijo.2012.1744

Abstract. Triple negative breast cancer (TNBC) has a poor outcome due to the lack of beneficial therapeutic targets. To clarify the molecular mechanisms involved in the carcinogenesis of TNBC and to identify target molecules for novel anticancer drugs, we analyzed the gene expression profiles of 30 TNBCs as well as 13 normal epithelial ductal cells that were purified by laser-microbeam microdissection. We identified 301 and 321 transcripts that were significantly upregulated and downregulated in TNBC, respectively. In particular, gene expression profile analyses of normal human vital organs allowed us to identify 104 cancer-specific genes, including those involved in breast carcinogenesis such as *NEK2*, *PBK* and *MELK*. Moreover, gene annotation enrichment analysis revealed prominent gene subsets involved in the cell cycle, especially mitosis. Therefore, we focused on cell cycle regulators, asp (abnormal spindle) homolog, microcephaly-associated (*Drosophila*) (*ASPM*) and centromere protein K (*CENPK*) as novel therapeutic targets for TNBC. Small-interfering RNA-mediated knockdown of their expression significantly attenuated TNBC cell viability due to G1 and G2/M cell cycle arrest. Our data will provide a better understanding of the

carcinogenesis of TNBC and could contribute to the development of molecular targets as a treatment for TNBC patients.

Introduction

Breast cancer is one of the most common solid malignant tumors among women worldwide. Breast cancer is a heterogeneous disease that is currently classified based on the expression of estrogen receptor (ER), progesterone receptor (PgR), and the human epidermal growth factor receptor 2 (HER2) (1,2). For patients with ER- or PgR-positive breast cancer, approximately five years of adjuvant endocrine therapy reduces the annual breast cancer death rate by approximately 30% (3). The addition of HER2-antagonist trastuzumab to adjuvant chemotherapy has improved the prognosis of HER2-positive breast cancer patients (4-6). In contrast, triple negative breast cancer (TNBC), defined as tumors that are negative for ER, PgR and HER2 overexpression, accounts for at least 15-20% of all breast cancers, and the prognosis for TNBC patients is poor because of its propensity for recurrence and metastasis and a lack of clinically-established targeted therapies (7,8). Therefore, only neoadjuvant chemotherapy with conventional cytotoxic agents yield an excellent outcome for TNBC patients who have a complete pathological response, but the outcome for the vast majority with residual disease after chemotherapy is relatively poor compared to non-TNBC patients (6,7). Thus, because the heterogeneity of breast cancer makes it difficult to treat many subtypes, including TNBC, the molecular mechanisms of the carcinogenesis of TNBC must be elucidated to develop novel molecular-targeted therapies that improve the clinical outcome of TNBC patients.

Current 'omics' technology including DNA microarray analysis can provide very helpful information that can be used to categorize the characteristics of various malignant tumors and identify genes that may be applicable for the develop-

Correspondence to: Dr Toyomasa Katagiri, Division of Genome Medicine, Institute of Genome Research, The University of Tokushima, 3-18-15 Kuramoto-cho, Tokushima 770-8503, Japan
E-mail: tkatagi@genome.tokushima-u.ac.jp

*Contributed equally

Key words: triple negative breast cancer, expression profiling, molecular targets

ment of novel molecular targets for therapeutic modalities (9). To this end, we analyzed the gene expression profile of 30 TNBC cells and normal breast ductal cells that were purified by laser-microbeam microdissection and identified a number of cancer-specific genes that might contribute to the carcinogenesis of TNBC. TNBC gene expression profiling analysis can provide comprehensive information on the molecular mechanism underlying the carcinogenesis of TNBC and possibly lead to the development of novel effective therapies.

Materials and methods

Clinical samples and cell lines. A total of 48 TNBC (18 cases did not entry DNA microarray analysis) and 13 normal mammary tissues were obtained with informed consent from patients who were treated at Tokushima Breast Care Clinic, Tokushima, Japan. This study, as well as the use of all clinical materials described above, was approved by the Ethics Committee of The University of Tokushima. Clinical information was obtained from medical records and tumors were diagnosed as triple-negative by pathologists when immunohistochemical staining was ER-negative, PR-negative, and HER2 (0 or 1+). The clinicopathological features of each patient are summarized in Table I. Samples were immediately embedded in TissueTek OCT compound (Sakura, Tokyo, Japan), frozen, and stored at -80°C . Human TNBC cell lines MDA-MB-231, BT-20, BT-549, HCC1143, and HCC1937 were purchased from the American Type Culture Collection (ATCC, Rockville, MD, USA). The human normal breast epithelial cell line, MCF10A, was purchased from Cambrex Bioscience, Inc. All cells were cultured under the conditions recommended by their respective depositors.

Laser-microbeam microdissection (LMM), RNA extraction, RNA amplification, and hybridization. Frozen specimens were serially sectioned in $8\text{-}\mu\text{m}$ slices with a cryostat (Leica, Herborn, Germany) and stained with hematoxylin and eosin to define the analyzed regions. We purified 48 TNBC and 13 normal ductal cells using the LMM system (Carl Zeiss, Jena, Germany) according to the manufacturer's instructions. Dissected cancer and normal ductal cells were dissolved in RLT lysis buffer (Qiagen, Valencia, CA, USA) containing 1% β -mercaptoethanol. The extracted total RNA was purified with an RNeasy Mini kit (Qiagen) according to the manufacturer's instructions. For RNA amplification and labeling, we used an Agilent Low-Input QuickAmp labeling kit according to the manufacturer's instructions. Briefly, 100 ng of total RNA from each sample was amplified using T7 RNA polymerase with simultaneous Cy3-labeled CTP incorporation. Then, $2\ \mu\text{g}$ of Cy3-labeled cRNA was fragmented, hybridized onto the Agilent Whole Human Genome Microarray 4x44K slide (Agilent Technologies, Palo Alto, CA, USA) and then incubated with rotation at 65°C for 18 h. Then slides were washed and scanned by the Agilent Microarray scanner system in an ozone protection fume hood.

Microarray analysis. The features of scanned image files containing the Cy3-fluorescence signals of the hybridized Agilent Microarrays were extracted using the Agilent Feature

Extraction (version 9.5) (Agilent Technologies). The data were analyzed using GeneSpring (version 11.5). We normalized the microarray data across all chips and genes by quantile normalization, and baseline transformed the signal values to the median in all samples. Finally, we performed quality control and filtering steps based on flags and expression levels. To identify genes that were significantly alternated between TNBC and normal ductal cells the mean signal intensity values in each analysis were compared. In this experiment, we applied Mann-Whitney (unpaired) t-test and random permutation test 10,000 times for each comparison and adjusted for multiple comparisons using the Benjamini Hochberg false discovery rate (FDR). Gene expression levels were considered significantly different when the FDR (corrected P-value) $<5 \times 10^{-4}$ (when comparing normal ductal cells and TNBC) and the fold change was ≥ 5.0 . Data from this microarray analysis has been submitted to the NCBI Gene Expression Omnibus (GEO) archive as series GSE38959.

Functional gene annotation clustering. The Database for Annotation, Visualization and Integrated Discovery (DAVID 6.7) was approved to detect functional gene annotation clusters based on gene expression profiling by gene annotation enrichment analysis (<http://david.abcc.ncifcrf.gov/>) (10,11). The clusters from the gene annotation enrichment analysis were selected in this study based on a previous report (12).

Quantitative reverse transcription-PCR (qRT-PCR) analysis. Total RNA was extracted from each TNBC cell line and clinical sample using an RNeasy mini kit (Qiagen) according to the manufacturer's instructions. Purified RNA from each clinical sample and cell line, as well as poly-A RNA from normal human heart, lung, liver, and kidney (Takara, Otsu, Japan) was reverse transcribed for single-stranded cDNA using oligo(dT)₁₂₋₁₈ primers with Superscript II reverse transcriptase (Invitrogen, Life Technologies, Carlsbad, CA, USA). qRT-PCR analysis was performed using an ABI PRISM 7500 Real-Time PCR system (Applied Biosystems, Life Technologies, Carlsbad, CA, USA) and SYBR Premix Ex Taq (Takara) according to the manufacturer's instructions. The PCR primer sequences were as follows: 5'-GCAGGTCTCC TTCCTTTGCT-3' and 5'-CTCGGCCTTCTTTGAGT GGT-3' for *ASPM*; 5'-CACTCACCGATTCAAATG CTC-3' and 5'-ACCACCGTTGTTCCCTTTCT-3' for *CENPK*; 5'-AAC TTAGAGGTGGGGAGCAG-3' and 5'-CACAAACCATGCC TTACTTTATC-3' for $\beta 2$ microglobulin ($\beta 2$ -MG) as a quantitative control.

Gene-silencing effect by RNA interference. Targeted sequences for *ASPM* and *CENPK* were determined using an siRNA Targeted Finder (Applied Biosystems, Life Technologies; http://www.ambion.com/techlib/misc/siRNA_finder.html). The siRNA targeting sequences were 5'-CATACAGAAGT GCGAGAAA-3' for *ASPM*, 5'-CTCAGTCAATGGC AGAAAA-3' for *CENPK* and 5'-GCAGCAGACTTCT TCAAG-3' for *EGFP* as a control siRNA. Human TNBC cell lines, HCC1937, MDA-MB-231 and BT-20, were plated at a density of 1×10^4 cells per well in 12-wells for the MTT assay and 3×10^4 cells per well in 6-well plates for flow cytometry and RT-PCR analyses. Cells were transfected with 16.6 nM

Table I. Clinicopathological features of 48 TNBC patients.

ID	Age	Histology	TNM	Stage	ER/PgR/HER2	Microarray	RT-PCR
1	44	Papillo-tubular	T0N3M1	IV	-/-/0	Done	Done
8	79	DCIS	T1N0M0	I	-/-/0	Not done	Done
10	57	Papillo-tubular	T1N0M0	I	-/-/1+	Not done	Done
19	63	Solid-tubular	T1N0M0	I	-/-/0	Not done	Done
27	60	Solid-tubular	T2N1M0	II	-/-/0	Done	Done
42	59	Solid-tubular	T2N0M0	II	-/-/0	Not done	Done
44	79	Papillo-tubular	Recurrence	-	-/-/1+	Not done	Done
53	55	Papillo-tubular	T1N0M0	I	-/-/0	Not done	Done
54	77	Solid-tubular	T1N1M0	II	-/-/0	Not done	Done
56	28	Scirrhou	T2N1M0	II	-/-/0	Done	Done
57	58	Solid-tubular	T1N1M0	II	-/-/0	Not done	Done
60	54	Solid-tubular	T2N1M0	II	-/-/0	Done	Done
64	60	Papillo-tubular	T2N0M0	II	-/-/0	Not done	Done
66	59	Special type	T2N1M0	II	-/-/0	Not done	Done
78	45	Solid-tubular	T2N1M0	II	-/-/0	Done	Done
89	44	Papillo-tubular	Recurrence	-	-/-/0	Not done	Done
95	60	Solid-tubular	T1N0M0	I	-/-/0	Not done	Done
101	60	Scirrhou	T2N1M0	II	-/-/0	Not done	Done
110	77	Scirrhou	T2N1M0	II	-/-/1+	Not done	Done
116	70	Solid-tubular	T2N1M0	II	-/-/0	Done	Done
155	36	Solid-tubular	T1N1M0	II	-/-/0	Done	Done
225	49	Papillo-tubular	T2N1M0	II	-/-/1+	Not done	Done
252	49	Solid-tubular	T2N1M0	II	-/-/1+	Done	Done
253	49	Scirrhou	T2N1M0	II	-/-/0	Done	Done
265	80	Scirrhou	T1N1M0	II	-/-/0-1+	Done	Done
313	53	Scirrhou	T3N2M0	III	-/-/0	Done	Done
337	42	Solid-tubular	T2N1M0	II	-/-/1+	Done	Done
359	55	Papillo-tubular	T2N0M0	II	-/-/0	Done	Done
362	37	Papillo-tubular	T2N1M0	II	-/-/0	Done	Done
363	69	Papillo-tubular	T2N0M0	II	-/-/0	Done	Done
366	61	Special type	T2N1M0	II	-/-/0-1+	Done	Done
384	32	Papillo-tubular	T3N0M0	II	-/-/0	Done	Done
392	46	Papillo-tubular	T1N1M0	II	-/-/0	Done	Done
414	60	Papillo-tubular	T2N1M0	II	-/-/1+	Not done	Done
415	54	Solid-tubular	T2N0M0	II	-/-/1+	Done	Done
420	41	Solid-tubular	T3N0M0	II	-/-/0	Done	Done
423	70	Solid-tubular	T2N0M0	II	-/-/0	Done	Done
438	63	Solid-tubular	T3N0M0	II	-/-/0	Done	Done
445	39	Solid-tubular	T2N1M0	II	-/-/0	Done	Done
453	50	Solid-tubular	T2N1M0	II	-/-/0	Done	Done
481	59	Solid-tubular	T3N1M0	III	-/-/0	Done	Done
528	55	Solid-tubular	T2N1M0	II	-/-/0	Done	Done
535	58	Solid-tubular	T2N1M0	II	-/-/0	Not done	Done
553	71	Solid-tubular	T0N1M0	II	-/-/1+	Not done	Done
558	56	Solid-tubular	T2N1M0	II	-/-/0	Done	Done
562	64	Scirrhou	T2N0M0	II	-/-/0	Done	Done
566	52	Solid-tubular	T3N1M0	III	-/-/0	Done	Done
651	45	Scirrhou	T2N1M0	II	-/-/0	Done	Done

DCIS, ductal carcinoma *in situ*; papillo-tubular, papillo-tubular adenocarcinoma; solid-tubular, solid-tubular adenocarcinoma; scirrhou, scirrhou carcinoma; special type ID 66, adenocarcinoma with squamous cell carcinoma; ID 366, osseous metaplasia; case 44, axillary lymph node metastasis was diagnosed 8 months after the first surgery followed by the dissection of metastatic lymph nodes; case 89, local recurrence in residual breast occurred after 2 years of the first surgery followed by a lumpectomy. All information was judged according to the General Rules for Clinical and Pathological Recording of Breast Cancer (The Japanese Breast Cancer Society). T, tumor stage; N, lymph node metastasis status; M, distant metastasis.

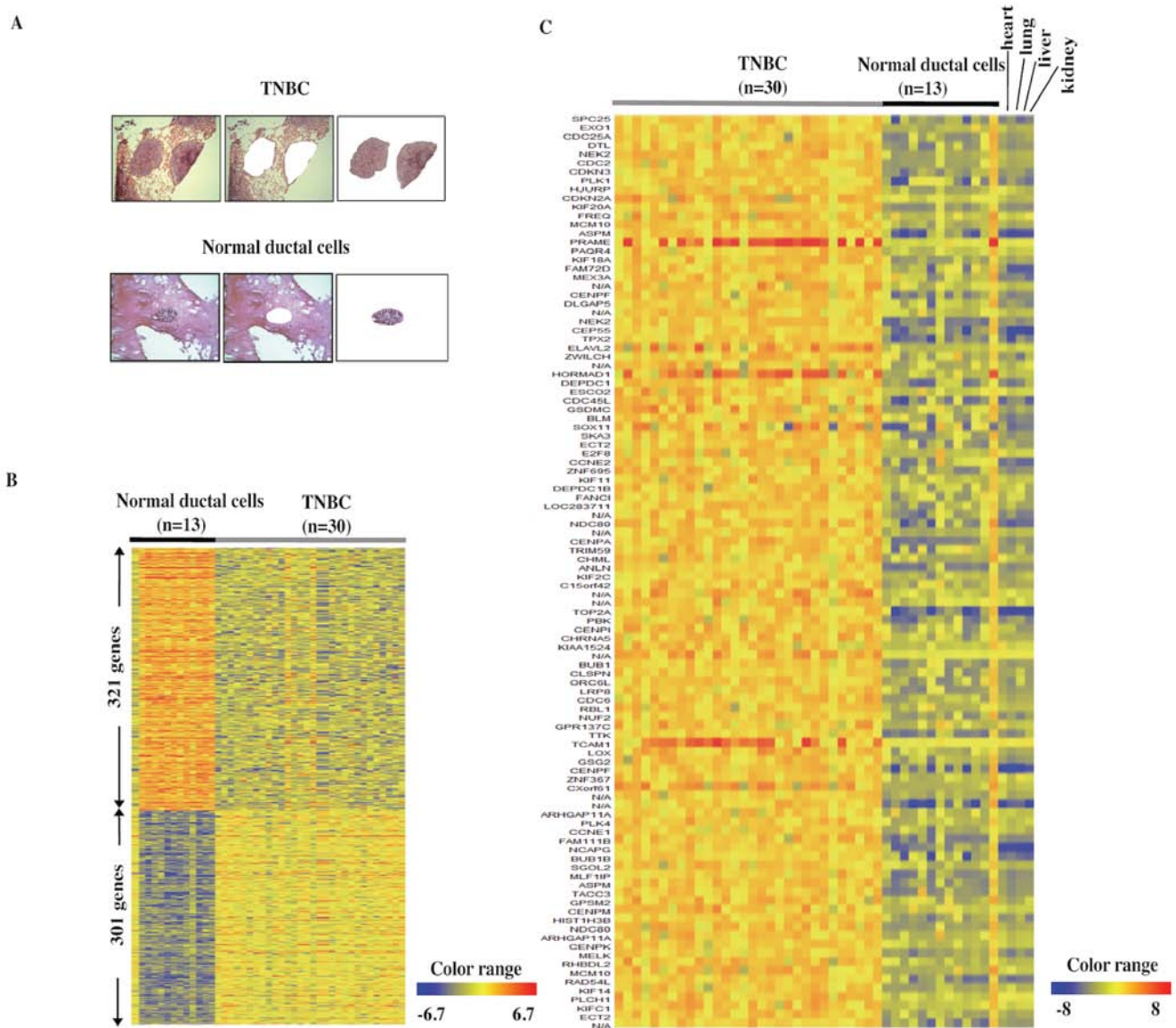


Figure 1. Purification of TNBC cells or ductal epithelial cells from normal ducts by means of microdissection and TNBC gene expression profiling. (A) Representative images of purified cancer cells and normal ductal epithelial cells from TNBC. Pre-microdissected (left lane), post-microdissected (middle lane) and microdissected cells (right lane) are shown after hematoxylin and eosin staining. (B) Heat-map image representing 622 genes that were significantly upregulated or downregulated >5-fold in TNBC. (C) Heat-map showing upregulated genes compared with normal ductal cells with no expression in normal organs including the heart, lung, liver and kidney.

of each siRNA using Lipofectamine RNAiMAX Reagent (Invitrogen). To evaluate the gene-silencing effects of the siRNAs by qRT-PCR, total RNA was extracted from the siRNA-transfected cells as described above after the indicated times. The following specific qRT-PCR primer sets were used: 5'-CGGAAAAGAAAGAGCGATGG-3' and 5'-ACCACCAAGTGAAGCCCTGT-3' for *ASPM* and 5'-GGGTGCCATCATTTTCTGGT-3' and 5'-CCACCGTTGTTCCCTTTCTAAG-3' for *CENPK*. To evaluate cell viability, the MTT assay was performed using the cell counting kit-8 reagent (Dojindo, Kumamoto, Japan) according to the manufacturer's instructions. Absorbance at 450 nm was measured with a micro-plate reader infinite 200 (Tecan, Männedorf, Switzerland). These experiments were performed in triplicate.

Colony formation assay. Vector-based shRNAs and the psiU6BX3 expression system were constructed as previously described (13). The shRNA target sequences were the same as those of the siRNA oligonucleotides. The DNA sequences of all constructs were confirmed by DNA sequencing. BT-20 and MDA-MB-231 cells were plated in 10-cm dishes (1×10^6 cells/dish) and transfected with 6 μ g of psiU6BX3.0-*ASPM* or psiU6BX3.0-*CENPK* and psiU6BX3.0-*EGFP* as a control using Fugene-6 (Roche, Basel, Switzerland) according to the manufacturer's instructions. Forty-eight hours after transfection, cells were re-seeded for a colony formation assay (5.0×10^5 cells/10-cm dish) and RT-PCR (5.0×10^5 cells/10-cm dish). We selected psiU6BX3.0-transfected cells using selection medium containing 0.6 mg/ml of neomycin for BT-20 cells and 1.4 mg/ml for MDA-MB-231 cells. Total

RNA was extracted from the cells after a 7-day incubation with neomycin, and then the knockdown effects of the siRNAs were examined by qRT-PCR. The specific primer sets for quantitative RT-PCR were the same as those for the siRNA oligonucleotides. Nineteen days after transfection, the cells were fixed with 4% paraformaldehyde for 10 min and stained with Giemsa solution (Merck, Darmstadt, Germany).

Cell cycle analysis. For flow cytometric analysis, adherent and detached cells were harvested and fixed with 70% ethanol at room temperature for 30 min. After washing with PBS (-), the cells were incubated at 37°C for 30 min with 1 mg/ml RNase I in PBS (-) and stained with 20 µg propidium iodide at room temperature for 30 min in the dark. A total of 10,000 cells were analyzed for DNA content using flow cytometry and CellQuest software (FACSCalibur; BD Biosciences, Franklin Lakes, NJ, USA). Assays were performed in duplicate.

Immunocytochemical staining analysis. HCC1937 and MDA-MB-231 cells were plated onto a 2-well glass slide (Thermo Fisher Scientific, Rochester, NY, USA) at a density of 1.0×10^4 /well and incubated for 24 h before siRNA transfection. Forty-eight hours post-transfection, the cells were fixed with 4% paraformaldehyde for 30 min at 4°C and then permeabilized with 0.1% Triton X-100 for 2 min at room temperature. Subsequently, the cells were covered with 3% bovine serum albumin for 60 min at room temperature and then incubated with an anti- α/β tubulin antibody (Cell Signaling, Beverly, MA, USA) diluted 1:50 for 1 h. After washing with PBS (-), the cells were stained with an Alexa 488-conjugated anti-rabbit secondary antibody (Molecular Probes, Eugene, OR, USA) diluted 1:1,000 for 1 h. The nuclei were counterstained with 4',6'-diamidino-2'-phenylindole dihydrochloride (DAPI). Fluorescent images were obtained using an IX71 microscope (Olympus, Tokyo, Japan).

Statistical analysis. Statistical significance was calculated by Mann-Whitney t-test using Stat View 5.0 J software (SAS Institute, Inc., Cary, NC, USA) to compare the gene expression levels between TNBC cells and normal ductal cells, and by Student's two-sided t-test using Microsoft® Excel 2008 to assess cell proliferation, gene expression, and alteration of cell cycle. A difference of $P < 0.05$ was considered statistically significant.

Results

Identification of genes upregulated or downregulated in TNBCs. To obtain precise expression profiles of TNBC cells, we used LMM to avoid contamination of non-cancer cells, such as adipocytes, fibroblasts, and inflammatory cells from the tissue sections (Fig. 1A, upper panels). Because breast cancer originates from normal breast ductal cells, we used similarly purified populations of normal duct cells as controls (Fig. 1A, lower panels). The precise gene-expression profiles of TNBC by DNA microarray identified 301 genes that were upregulated >5-fold in TNBC compared to 13 normal ductal cells, and 321 genes that were downregulated to <1/5 of the normal ductal cells (Fig. 1B). Table II lists the 301 upregulated genes in TNBC, including ubiquitin-conjugating enzyme E2C (*UBE2C*)

(14), S100 calcium binding protein P (*S100P*) (15), ubiquitin carboxyl-terminal esterase L1 (ubiquitin thiolesterase) (*UCHL1*) (16), pituitary tumor-transforming 1 (*PTTGI*) (17), ubiquitin-conjugating enzyme E2T (*UBE2T*) (13), ubiquitin-like with PHD and ring finger domains 1 (*UHRF1*) (18), SIX homeobox 1 (*SIX1*) (19), and protein regulator of cytokinesis 1 (*PRCI*) (20), which were previously reported to be overexpressed in breast cancer and involved in mammary carcinogenesis. In particular, topoisomerase (DNA) II α (*TOP2A*) (21,22), HORMA domain containing 1 (*HORMAD1*) (23), ATPase family, Fatty acid binding protein 5 (psoriasis-associated) (*FABP5*) (24), and AAA domain containing 2 (*ATAD2*) (25) were previously reported to be potentially involved in the carcinogenesis of TNBC, and to serve as prognostic markers or therapeutic targets for TNBC.

On the other hand, Table III lists the 321 genes that were downregulated to <1/5 of normal ductal cells. Among these significantly downregulated genes, prolactin-induced protein (*PIP*) and dynein, axonemal, light intermediate chain 1 (*DNAL1*) were previously shown to be downregulated in TNBC (26). In particular, suppression of WNT inhibitory factor 1 (*WIF1*) (27) and signal peptide, CUB domain, EGF-like (*SCUBE2*) (28), both of which function as tumor suppressors, were among the genes that were downregulated as malignancy progressed. These data suggest that silencing or depletion of these genes might lead to the carcinogenesis of TNBC.

Identification of cancer-specific genes. Next, to develop novel therapeutic targets for TNBC with a minimum risk of adverse events, we performed a DNA microarray analysis of normal human vital organs consisting of the heart, lung, liver and kidney as well as TNBC cases and attempted to identify genes whose expression was exclusively upregulated in TNBC, but not expressed in normal vital organs. We identified 104 genes, which were specifically upregulated in TNBC, including cancer-specific molecules such as NIMA-related kinase 2 (*NEK2*) (29,30), PDZ binding kinase (*PBK*) (31), denticleless homolog (*Drosophila*) (*DTL*) (32), maternal leucine zipper kinase (*MELK*) (33), and kinesin family member C (*KIF2C*) (34), which have previously been shown to be involved in breast carcinogenesis (Fig. 1C and Table IV).

Functional gene annotation clustering analysis. To elucidate the biological processes and pathways characterized in TNBC, we performed a functional analysis of these upregulated or downregulated genes in 30 TNBC cases using the gene annotation clustering of the DAVID algorithm. We identified the most prominent cluster (cluster 1; gene enrichment score, 29.90) composed of various functional annotation terms consisting of 87 upregulated genes in TNBC (Table V). Cluster 1 consisted almost entirely of cell cycle-associated genes as represented by nuclear division (fold enrichment, 15.04), mitosis (fold enrichment, 15.04), M phase of the mitotic cell cycle (fold enrichment, 14.78), organelle fission (fold enrichment, 14.45), and M phase (fold enrichment, 12.90) (Fig. 2). These findings suggest that most of the upregulated genes in TNBC might be functionally responsible for cell cycle progression.

On the other hand, we also identified the most prominent cluster functionally deactivated in TNBC based on down-

Table II. Genes significantly upregulated in TNBC compared with normal ductal cells.

Probe ID	Accession no.	Symbol	Gene name	Fold change (log)	P-value
A_24_P334130	NM_054034	<i>FNI</i>	Fibronectin 1	5.33	1.26E-04
A_24_P940678	N/A	N/A		5.07	1.26E-04
A_23_P367618	NM_003412	<i>ZIC1</i>	Zic family member 1 (odd-paired homolog, <i>Drosophila</i>)	5.01	1.26E-04
A_23_P118834	NM_001067	<i>TOP2A</i>	Topoisomerase (DNA) II α 170 kDa	4.76	1.26E-04
A_32_P119154	BE138567	N/A		4.75	1.26E-04
A_23_P35219	NM_002497	<i>NEK2</i>	NIMA (never in mitosis gene a)-related kinase 2	4.67	1.26E-04
A_23_P166360	NM_206956	<i>PRAME</i>	Preferentially expressed antigen in melanoma	4.64	1.26E-04
A_24_P332314	NM_198947	<i>FAM111B</i>	Family with sequence similarity 111, member B	4.63	1.26E-04
A_24_P413884	NM_001809	<i>CENPA</i>	Centromere protein A	4.59	1.26E-04
A_23_P68610	NM_012112	<i>TPX2</i>	TPX2, microtubule-associated, homolog (<i>Xenopus laevis</i>)	4.58	1.26E-04
A_23_P58266	NM_005980	<i>S100P</i>	S100 calcium binding protein P	4.57	1.26E-04
A_24_P297539	NM_181803	<i>UBE2C</i>	Ubiquitin-conjugating enzyme E2C	4.49	1.26E-04
A_23_P401	NM_016343	<i>CENPF</i>	Centromere protein F, 350/400 ka (mitosin)	4.44	1.26E-04
A_23_P57379	NM_003504	<i>CDC45L</i>	CDC45 cell division cycle 45-like (<i>S. cerevisiae</i>)	4.44	1.26E-04
A_23_P118815	NM_001012271	<i>BIRC5</i>	Baculoviral IAP repeat-containing 5	4.43	1.26E-04
A_23_P210853	NM_021067	<i>GINS1</i>	GINS complex subunit 1 (Psf1 homolog)	4.41	1.26E-04
A_23_P258493	NM_005573	<i>LMNB1</i>	Lamin B1	4.31	1.26E-04
A_24_P119745	NM_212482	<i>FNI</i>	Fibronectin 1	4.31	1.26E-04
A_24_P680947	BC044933	<i>KIF18B</i>	Kinesin family member 18B	4.3	1.26E-04
A_32_P92642	N/A	N/A		4.3	1.26E-04
A_23_P356684	NM_018685	<i>ANLN</i>	Anillin, actin binding protein	4.29	1.26E-04
A_24_P314571	BU616832	N/A		4.24	1.26E-04
A_23_P98580	NM_004265	<i>FADS2</i>	Fatty acid desaturase 2	4.2	1.26E-04
A_23_P52017	NM_018136	<i>ASPM</i>	asp (abnormal spindle) homolog, microcephaly associated (<i>Drosophila</i>)	4.17	1.26E-04
A_24_P20607	NM_005409	<i>CXCL11</i>	Chemokine (C-X-C motif) ligand 11	4.16	2.33E-04
A_32_P199884	NM_032132	<i>HORMAD1</i>	HORMA domain containing 1	4.13	2.33E-04
A_23_P70007	NM_012484	<i>HMMR</i>	Hyaluronan-mediated motility receptor (RHAMM)	4.11	1.26E-04
A_23_P22378	NM_003108	<i>SOX11</i>	SRY (sex determining region Y)-box 11	4.1	1.26E-04
A_23_P259586	NM_003318	<i>TTK</i>	TTK protein kinase	4.09	1.26E-04
A_23_P200310	NM_017779	<i>DEPDC1</i>	DEP domain containing 1	4.08	1.26E-04
A_24_P378331	NM_170589	<i>CASC5</i>	Cancer susceptibility candidate 5	4.06	1.26E-04
A_23_P111888	NM_138455	<i>CTHRC1</i>	Collagen triple helix repeat containing 1	4.05	1.26E-04
A_23_P48835	NM_138555	<i>KIF23</i>	Kinesin family member 23	4.05	1.26E-04
A_23_P115872	NM_018131	<i>CEP55</i>	Centrosomal protein 55 kDa	4.03	1.26E-04
A_23_P132956	NM_004181	<i>UCHL1</i>	Ubiquitin carboxyl-terminal esterase L1 (ubiquitin thiolesterase)	4.03	1.26E-04
A_24_P911179	NM_018136	<i>ASPM</i>	asp (abnormal spindle) homolog, microcephaly associated (<i>Drosophila</i>)	4.02	1.26E-04
A_23_P408955	NM_004091	<i>E2F2</i>	E2F transcription factor 2	4.02	1.26E-04
A_23_P7636	NM_004219	<i>PTTG1</i>	Pituitary tumor-transforming 1	4	1.26E-04
A_23_P204941	NM_004004	<i>GJB2</i>	Gap junction protein, β 2, 26 kDa	4	1.26E-04
A_23_P18452	NM_002416	<i>CXCL9</i>	Chemokine (C-X-C motif) ligand 9	3.94	2.33E-04
A_24_P96780	NM_016343	<i>CENPF</i>	Centromere protein F, 350/400 ka (mitosin)	3.92	1.26E-04
A_23_P69537	NM_006681	<i>NMU</i>	Neuromedin U	3.9	1.26E-04

Table II. Continued.

Probe ID	Accession no.	Symbol	Gene name	Fold change (log)	P-value
A_24_P14156	NM_006101	<i>NDC80</i>	<i>NDC80</i> homolog, kinetochore complex component (<i>S. cerevisiae</i>)	3.86	1.26E-04
A_23_P254733	NM_024629	<i>MLF1IP</i>	MLF1 interacting protein	3.85	1.26E-04
A_23_P74115	NM_003579	<i>RAD54L</i>	RAD54-like (<i>S. cerevisiae</i>)	3.84	1.26E-04
A_23_P50108	NM_006101	<i>NDC80</i>	<i>NDC80</i> homolog, kinetochore complex component (<i>S. cerevisiae</i>)	3.84	1.26E-04
A_24_P150160	NM_004265	<i>FADS2</i>	Fatty acid desaturase 2	3.83	1.26E-04
A_23_P155815	NM_022346	<i>NCAPG</i>	Non-SMC condensin I complex, subunit G	3.82	1.26E-04
A_23_P125278	NM_005409	<i>CXCL11</i>	Chemokine (C-X-C motif) ligand 11	3.81	1.26E-04
A_23_P51085	NM_020675	<i>SPC25</i>	SPC25, <i>NDC80</i> kinetochore complex component, homolog (<i>S. cerevisiae</i>)	3.81	1.26E-04
A_23_P133123	NM_032117	<i>MND1</i>	Meiotic nuclear divisions 1 homolog (<i>S. cerevisiae</i>)	3.8	1.26E-04
A_32_P62997	NM_018492	<i>PBK</i>	PDZ binding kinase	3.8	1.26E-04
A_23_P256956	NM_005733	<i>KIF20A</i>	Kinesin family member 20A	3.79	1.26E-04
A_24_P933613	N/A	N/A		3.78	1.26E-04
A_23_P212844	NM_006342	<i>TACC3</i>	Transforming, acidic coiled-coil containing protein 3	3.78	1.26E-04
A_24_P254705	NM_020394	<i>ZNF695</i>	Zinc finger protein 695	3.76	1.26E-04
A_23_P115482	NM_014176	<i>UBE2T</i>	Ubiquitin-conjugating enzyme E2T (putative)	3.75	1.26E-04
A_32_P201723	N/A	N/A		3.73	1.26E-04
A_23_P256425	NM_014479	<i>ADAMDEC1</i>	ADAM-like, decysin 1	3.73	1.26E-04
A_23_P432352	NM_001017978	<i>CXorf61</i>	Chromosome X open reading frame 61	3.73	1.26E-04
A_23_P208880	NM_013282	<i>UHRF1</i>	Ubiquitin-like with PHD and ring finger domains 1	3.72	1.26E-04
A_23_P323751	NM_030919	<i>FAM83D</i>	Family with sequence similarity 83, member D	3.71	1.26E-04
A_23_P48669	NM_005192	<i>CDKN3</i>	Cyclin-dependent kinase inhibitor 3	3.71	1.26E-04
A_24_P234196	NM_001034	<i>RRM2</i>	Ribonucleotide reductase M2	3.69	1.26E-04
A_23_P253791	NM_004345	<i>CAMP</i>	Cathelicidin antimicrobial peptide	3.69	1.26E-04
A_23_P76914	NM_005982	<i>SIX1</i>	SIX homeobox 1	3.67	4.43E-04
A_23_P94571	NM_004432	<i>ELAVL2</i>	ELAV (embryonic lethal, abnormal vision, <i>Drosophila</i>)-like 2 (Hu antigen B)	3.67	1.26E-04
A_23_P200222	NM_033300	<i>LRP8</i>	Low density lipoprotein receptor-related protein 8, apolipoprotein E receptor	3.67	1.26E-04
A_24_P416079	NM_016359	<i>NUSAP1</i>	Nucleolar and spindle associated protein 1	3.66	1.26E-04
A_23_P104651	NM_080668	<i>CDCA5</i>	Cell division cycle associated 5	3.65	1.26E-04
A_23_P150667	NM_031217	<i>KIF18A</i>	Kinesin family member 18A	3.64	1.26E-04
A_24_P859859	N/A	N/A		3.63	4.43E-04
A_23_P312150	NM_001956	<i>EDN2</i>	Endothelin 2	3.61	1.26E-04
A_23_P375	NM_018101	<i>CDCA8</i>	Cell division cycle associated 8	3.59	1.26E-04
A_32_P68525	BC035392	N/A		3.58	1.26E-04
A_23_P43490	NM_058197	<i>CDKN2A</i>	Cyclin-dependent kinase inhibitor 2A (melanoma, p16, inhibits CDK4)	3.56	1.26E-04
A_23_P1691	NM_002421	<i>MMP1</i>	Matrix metalloproteinase 1 (interstitial collagenase)	3.55	1.26E-04
A_23_P117852	NM_014736	<i>KIAA0101</i>	KIAA0101	3.54	1.26E-04
A_24_P319613	NM_002497	<i>NEK2</i>	NIMA (never in mitosis gene a)-related kinase 2	3.53	1.26E-04
A_23_P10385	NM_016448	<i>DTL</i>	Denticleless homolog (<i>Drosophila</i>)	3.53	1.26E-04

Table II. Continued.

Probe ID	Accession no.	Symbol	Gene name	Fold change (log)	P-value
A_32_P1173	NM_138441	<i>C6orf150</i>	Chromosome 6 open reading frame 150	3.51	1.26E-04
A_23_P94422	NM_014791	<i>MELK</i>	Maternal embryonic leucine zipper kinase	3.5	1.26E-04
A_23_P340909	BC013418	<i>SKA3</i>	Spindle and kinetochore associated complex subunit 3	3.48	1.26E-04
A_23_P385861	NM_152562	<i>CDCA2</i>	Cell division cycle associated 2	3.47	1.26E-04
A_23_P124417	NM_004336	<i>BUB1</i>	Budding uninhibited by benzimidazoles 1 homolog (yeast)	3.47	1.26E-04
A_24_P257099	NM_018410	<i>HJURP</i>	Holliday junction recognition protein	3.43	1.26E-04
A_24_P270460	NM_005532	<i>IFI27</i>	Interferon, α -inducible protein 27	3.41	2.33E-04
A_23_P206059	NM_003981	<i>PRC1</i>	Protein regulator of cytokinesis 1	3.39	1.26E-04
A_23_P74349	NM_145697	<i>NUF2</i>	NUF2, NDC80 kinetochore complex component, homolog (<i>S. cerevisiae</i>)	3.36	1.26E-04
A_24_P302584	NM_003108	<i>SOX11</i>	SRY (sex determining region Y)-box 11	3.36	4.43E-04
A_24_P68088	NR_002947	<i>TCAM1</i>	Testicular cell adhesion molecule 1 homolog (mouse)	3.35	2.33E-04
A_24_P605612	NM_003247	<i>THBS2</i>	Thrombospondin 2	3.34	1.26E-04
A_24_P366033	NM_018098	<i>ECT2</i>	Epithelial cell transforming sequence 2 oncogene	3.34	1.26E-04
A_23_P93258	NM_003537	<i>HIST1H3B</i>	Histone cluster 1, H3b	3.33	1.26E-04
A_23_P211762	N/A	<i>COL8A1</i>	Collagen, type VIII, α 1	3.29	4.43E-04
A_23_P77493	NM_006086	<i>TUBB3</i>	Tubulin, β 3	3.29	1.26E-04
A_23_P204947	NM_004004	<i>GJB2</i>	Gap junction protein, β 2, 26 kDa	3.29	1.26E-04
A_23_P149668	NM_014875	<i>KIF14</i>	Kinesin family member 14	3.29	1.26E-04
A_23_P34325	NM_033300	<i>LRP8</i>	Low density lipoprotein receptor-related protein 8, apolipoprotein E receptor	3.28	1.26E-04
A_32_P56154	N/A	N/A		3.28	1.26E-04
A_32_P10403	BU618641	<i>SERPINE1</i>	Serpin peptidase inhibitor, clade E (nexin, plasminogen activator inhibitor type 1), member 1	3.27	1.26E-04
A_23_P138507	NM_001786	<i>CDC2</i>	Cell division cycle 2, G1→S and G2→M	3.24	1.26E-04
A_23_P48513	NM_005532	<i>IFI27</i>	Interferon, α -inducible protein 27	3.23	1.26E-04
A_23_P49972	NM_001254	<i>CDC6</i>	Cell division cycle 6 homolog (<i>S. cerevisiae</i>)	3.22	1.26E-04
A_24_P306896	XR_040656	<i>LOC283711</i>	Hypothetical protein LOC283711	3.22	1.26E-04
A_23_P44684	NM_018098	<i>ECT2</i>	Epithelial cell transforming sequence 2 oncogene	3.21	1.26E-04
A_24_P161773	N/A	N/A		3.2	1.26E-04
A_23_P100344	NM_014321	<i>ORC6L</i>	Origin recognition complex, subunit 6 like (yeast)	3.2	1.26E-04
A_32_P162183	NM_000063	<i>C2</i>	Complement component 2	3.18	1.26E-04
A_23_P163481	NM_001211	<i>BUB1B</i>	Budding uninhibited by benzimidazoles 1 homolog β (yeast)	3.17	1.26E-04
A_32_P113784	N/A	N/A		3.16	1.26E-04
A_32_P87849	N/A	N/A		3.16	1.26E-04
A_24_P397107	NM_001789	<i>CDC25A</i>	Cell division cycle 25 homolog A (<i>S. pombe</i>)	3.15	1.26E-04
A_23_P209200	NM_001238	<i>CCNE1</i>	Cyclin E1	3.15	1.26E-04
A_32_P16625	N/A	N/A		3.15	1.26E-04
A_23_P58321	NM_001237	<i>CCNA2</i>	Cyclin A2	3.15	1.26E-04
A_24_P37903	N/A	<i>LOX</i>	Lysyl oxidase	3.12	1.26E-04

Table II. Continued.

Probe ID	Accession no.	Symbol	Gene name	Fold change (log)	P-value
A_32_P64919	NM_001042517	<i>DIAPH3</i>	Diaphanous homolog 3 (<i>Drosophila</i>)	3.12	1.26E-04
A_23_P379614	NM_007280	<i>OIP5</i>	Opa interacting protein 5	3.12	1.26E-04
A_23_P206441	NM_000135	<i>FANCA</i>	Fanconi anemia, complementation group A	3.09	1.26E-04
A_23_P16915	NM_012413	<i>QPCT</i>	Glutaminyl-peptide cyclotransferase	3.09	1.26E-04
A_23_P137173	NM_021992	<i>TMSB15A</i>	Thymosin β 15a	3.07	1.26E-04
A_24_P313504	NM_005030	<i>PLK1</i>	Polo-like kinase 1 (<i>Drosophila</i>)	3.07	1.26E-04
A_23_P251421	NM_031942	<i>CDCA7</i>	Cell division cycle associated 7	3.06	1.26E-04
A_23_P252292	NM_006733	<i>CENPI</i>	Centromere protein I	3.04	1.26E-04
A_23_P158725	NM_001042422	<i>SLC16A3</i>	Solute carrier family 16, member 3 (monocarboxylic acid transporter 4)	3.04	1.26E-04
A_23_P57417	NM_005940	<i>MMP11</i>	Matrix metalloproteinase 11 (stromelysin 3)	3.03	1.26E-04
A_24_P291044	N/A	N/A		3.02	1.26E-04
A_23_P343927	NM_175065	<i>HIST2H2AB</i>	Histone cluster 2, H2ab	3.01	1.26E-04
A_23_P63789	NM_032997	<i>ZWINT</i>	ZW10 interactor	3.01	1.26E-04
A_23_P123596	NM_000170	<i>GLDC</i>	Glycine dehydrogenase (decarboxylating)	3	1.26E-04
A_23_P88731	NM_002875	<i>RAD51</i>	RAD51 homolog (RecA homolog, <i>E. coli</i>) (<i>S. cerevisiae</i>)	3	1.26E-04
A_23_P161474	NM_182751	<i>MCM10</i>	Minichromosome maintenance complex component 10	2.99	1.26E-04
A_24_P303354	NM_021064	<i>HIST1H2AG</i>	Histone cluster 1, H2ag	2.98	1.26E-04
A_23_P10518	NM_016521	<i>TFDP3</i>	Transcription factor Dp family, member 3	2.98	1.26E-04
A_24_P247660	NM_001002033	<i>HNI</i>	Hematological and neurological expressed 1	2.97	1.26E-04
A_23_P134910	NM_003878	<i>GGH</i>	γ -glutamyl hydrolase (conjugase, folylpolymagglutamyl hydrolase)	2.97	1.26E-04
A_32_P7193	N/A	N/A		2.97	1.26E-04
A_23_P49878	NM_019013	<i>FAM64A</i>	Family with sequence similarity 64, member A	2.96	1.26E-04
A_24_P359231	BC014312	<i>HIST1H2BJ</i>	Histone cluster 1, H2bj	2.95	1.26E-04
A_32_P140262	N/A	N/A		2.95	1.26E-04
A_23_P55270	NM_002988	<i>CCL18</i>	Chemokine (C-C motif) ligand 18 (pulmonary and activation-regulated)	2.95	1.26E-04
A_24_P462899	NM_001012507	<i>C6orf173</i>	Chromosome 6 open reading frame 173	2.94	1.26E-04
A_23_P502520	NM_172374	<i>IL4I1</i>	Interleukin 4 induced 1	2.94	1.26E-04
A_23_P253762	N/A	N/A		2.94	1.26E-04
A_23_P214908	AY374131	N/A		2.94	1.26E-04
A_24_P225534	NM_017821	<i>RHBDL2</i>	Rhomboid, veinlet-like 2 (<i>Drosophila</i>)	2.94	1.26E-04
A_23_P203419	NM_013402	<i>FADS1</i>	Fatty acid desaturase 1	2.94	1.26E-04
A_23_P150935	NM_005480	<i>TROAP</i>	Trophinin associated protein (tastin)	2.94	1.26E-04
A_24_P412088	NM_182751	<i>MCM10</i>	Minichromosome maintenance complex component 10	2.94	1.26E-04
A_23_P71727	NM_001827	<i>CKS2</i>	CDC28 protein kinase regulatory subunit 2	2.93	1.26E-04
A_23_P217236	NM_005342	<i>HMGB3</i>	High-mobility group box 3	2.92	1.26E-04
A_32_P109296	NM_152259	<i>C15orf42</i>	Chromosome 15 open reading frame 42	2.91	1.26E-04
A_23_P89509	NM_006461	<i>SPAG5</i>	Sperm associated antigen 5	2.91	1.26E-04
A_24_P563068	N/A	N/A		2.91	1.26E-04
A_23_P416468	NM_025049	<i>PIF1</i>	PIF1 5'-to-3' DNA helicase homolog (<i>S. cerevisiae</i>)	2.91	1.26E-04
A_24_P38895	NM_002105	<i>H2AFX</i>	H2A histone family, member X	2.9	1.26E-04
A_23_P52278	NM_004523	<i>KIF11</i>	Kinesin family member 11	2.89	1.26E-04
A_24_P144543	N/A	N/A		2.89	1.26E-04

Table II. Continued.

Probe ID	Accession no.	Symbol	Gene name	Fold change (log)	P-value
A_24_P71468	NM_012413	<i>QPCT</i>	Glutaminyl-peptide cyclotransferase	2.88	2.33E-04
A_23_P116123	NM_001274	<i>CHEK1</i>	CHK1 checkpoint homolog (S. pombe)	2.88	1.26E-04
A_32_P106235	N/A	N/A		2.87	1.26E-04
A_24_P139152	AL359062	<i>COL8A1</i>	Collagen, type VIII, α 1	2.87	4.43E-04
A_23_P36831	NM_003979	<i>GPRC5A</i>	G protein-coupled receptor, family C, group 5, member A	2.87	1.26E-04
A_23_P387471	NM_005931	<i>MICB</i>	MHC class I polypeptide-related sequence B	2.85	1.26E-04
A_23_P9574	NM_018098	<i>ECT2</i>	Epithelial cell transforming sequence 2 oncogene	2.84	1.26E-04
A_24_P535256	AK001903	<i>INHBA</i>	Inhibin, β A	2.84	1.26E-04
A_24_P76521	AK056691	<i>GSG2</i>	germ cell associated 2 (haspin)	2.83	1.26E-04
A_23_P103795	NM_138959	<i>VANGL1</i>	vang-like 1 (van gogh, <i>Drosophila</i>)	2.83	1.26E-04
A_32_P74409	NM_001145033	<i>LOC387763</i>	Hypothetical protein LOC387763	2.83	1.26E-04
A_23_P100632	NM_001002033	<i>HNI</i>	Hematological and neurological expressed 1	2.83	1.26E-04
A_23_P126212	NM_022111	<i>CLSPN</i>	Claspin homolog (<i>Xenopus laevis</i>)	2.83	1.26E-04
A_24_P659113	NM_152523	<i>CCNYL1</i>	Cyclin Y-like 1	2.83	1.26E-04
A_24_P367227	NM_001144755	<i>MYBL1</i>	v-myb myeloblastosis viral oncogene homolog (avian)-like 1	2.82	1.26E-04
A_23_P162719	NM_030932	<i>DIAPH3</i>	Diaphanous homolog 3 (<i>Drosophila</i>)	2.81	1.26E-04
A_32_P221799	NM_003514	<i>HIST1H2AM</i>	Histone cluster 1, H2am	2.81	1.26E-04
A_23_P60120	NM_031415	<i>GSDMC</i>	Gasdermin C	2.81	2.33E-04
A_24_P902509	NM_018193	<i>FANCI</i>	Fanconi anemia, complementation group I	2.8	1.26E-04
A_23_P50096	NM_001071	<i>TYMS</i>	Thymidylate synthetase	2.79	1.26E-04
A_32_P143245	NM_001012507	<i>C6orf173</i>	Chromosome 6 open reading frame 173	2.79	1.26E-04
A_23_P155969	NM_014264	<i>PLK4</i>	Polo-like kinase 4 (<i>Drosophila</i>)	2.79	1.26E-04
A_23_P62021	N/A	N/A		2.78	1.26E-04
A_32_P183218	NM_153695	<i>ZNF367</i>	Zinc finger protein 367	2.77	1.26E-04
A_23_P46118	NM_001821	<i>CHML</i>	Choroideremia-like (Rab escort protein 2)	2.76	2.33E-04
A_23_P327643	N/A	N/A		2.75	1.26E-04
A_23_P375104	NM_018193	<i>FANCI</i>	Fanconi anemia, complementation group I	2.75	1.26E-04
A_23_P1823	NM_000280	<i>PAX6</i>	Paired box 6	2.75	1.26E-04
A_23_P168014	NM_021066	<i>HIST1H2AJ</i>	Histone cluster 1, H2aj	2.74	1.26E-04
A_24_P413126	NM_020182	<i>PMEPA1</i>	Prostate transmembrane protein, androgen induced 1	2.74	1.26E-04
A_23_P80032	NM_005225	<i>E2F1</i>	E2F transcription factor 1	2.74	1.26E-04
A_23_P215976	NM_057749	<i>CCNE2</i>	Cyclin E2	2.72	2.33E-04
A_32_P231415	AF132203	<i>SCD</i>	Stearoyl-CoA desaturase (δ -9-desaturase)	2.72	1.26E-04
A_23_P370989	NM_005914	<i>MCM4</i>	Minichromosome maintenance complex component 4	2.72	1.26E-04
A_23_P216429	NM_017680	<i>ASPN</i>	Asporin	2.71	1.26E-04
A_24_P195621	NR_027288	<i>LOC341056</i>	SUMO-1 activating enzyme subunit 1 pseudogene	2.71	1.26E-04
A_32_P151800	NM_207418	<i>FAM72D</i>	Family with sequence similarity 72, member D	2.7	1.26E-04
A_23_P122197	NM_031966	<i>CCNB1</i>	Cyclin B1	2.7	1.26E-04
A_23_P34788	NM_006845	<i>KIF2C</i>	Kinesin family member 2C	2.7	1.26E-04
A_32_P206698	NM_001826	<i>CKS1B</i>	CDC28 protein kinase regulatory subunit 1B	2.7	1.26E-04
A_23_P99292	NM_006479	<i>RAD51AP1</i>	RAD51 associated protein 1	2.7	1.26E-04
A_23_P133956	NM_002263	<i>KIFC1</i>	Kinesin family member C1	2.69	1.26E-04
A_32_P143496	N/A	N/A		2.69	1.26E-04
A_32_P163858	NM_005063	<i>SCD</i>	Stearoyl-CoA desaturase (δ -9-desaturase)	2.69	1.26E-04

Table II. Continued.

Probe ID	Accession no.	Symbol	Gene name	Fold change (log)	P-value
A_32_P175557	R01145	N/A		2.69	1.26E-04
A_23_P63618	NM_005063	<i>SCD</i>	Stearoyl-CoA desaturase (δ -9-desaturase)	2.69	1.26E-04
A_23_P88630	NM_000057	<i>BLM</i>	Bloom syndrome, RecQ helicase-like	2.68	1.26E-04
A_24_P276102	NM_183404	<i>RBL1</i>	Retinoblastoma-like 1 (p107)	2.68	1.26E-04
A_23_P135385	N/A	N/A		2.68	1.26E-04
A_23_P57658	NM_020386	<i>HRASLS</i>	HRAS-like suppressor	2.67	1.26E-04
A_23_P23303	NM_003686	<i>EXO1</i>	Exonuclease 1	2.67	1.26E-04
A_23_P88691	NM_000745	<i>CHRNA5</i>	Cholinergic receptor, nicotinic, α 5	2.67	1.26E-04
A_24_P923381	NR_002219	<i>EPR1</i>	Effector cell peptidase receptor 1 (non-protein coding)	2.66	1.26E-04
A_23_P24444	NM_001360	<i>DHCR7</i>	7-dehydrocholesterol reductase	2.65	1.26E-04
A_23_P43157	NM_001080416	<i>MYBL1</i>	v-myb myeloblastosis viral oncogene homolog (avian)-like 1	2.65	2.33E-04
A_23_P88740	NM_018455	<i>CENPN</i>	Centromere protein N	2.64	1.26E-04
A_23_P131866	NM_198433	<i>AURKA</i>	Aurora kinase A	2.64	1.26E-04
A_23_P259641	NM_004456	<i>EZH2</i>	Enhancer of zeste homolog 2 (<i>Drosophila</i>)	2.64	1.26E-04
A_32_P72341	NM_173084	<i>TRIM59</i>	Tripartite motif-containing 59	2.62	1.26E-04
A_24_P227091	NM_004523	<i>KIF11</i>	Kinesin family member 11	2.61	1.26E-04
A_23_P145238	NM_080593	<i>HIST1H2BK</i>	Histone cluster 1, H2bk	2.61	1.26E-04
A_23_P136805	NM_014783	<i>ARHGAP11A</i>	Rho GTPase activating protein 11A	2.6	1.26E-04
A_23_P167997	NM_003518	<i>HIST1H2BG</i>	Histone cluster 1, H2bg	2.6	1.26E-04
A_23_P63402	NM_013296	<i>GPSM2</i>	G-protein signaling modulator 2 (AGS3-like, <i>C. elegans</i>)	2.6	1.26E-04
A_24_P192994	NM_013402	<i>FADS1</i>	Fatty acid desaturase 1	2.59	1.26E-04
A_23_P25559	NM_005845	<i>ABCC4</i>	ATP-binding cassette, sub-family C (CFTR/MRP), member 4	2.59	3.41E-04
A_23_P309381	NM_001040874	<i>HIST2H2AA4</i>	Histone cluster 2, H2aa4	2.59	1.26E-04
A_23_P35871	NM_024680	<i>E2F8</i>	E2F transcription factor 8	2.58	1.26E-04
A_23_P207307	N/A	N/A		2.58	1.26E-04
A_24_P399888	NM_001002876	<i>CENPM</i>	Centromere protein M	2.58	1.26E-04
A_23_P360754	NM_005099	<i>ADAMTS4</i>	ADAM metallopeptidase with thrombospondin type 1 motif, 4	2.57	3.41E-04
A_23_P21706	NM_001905	<i>CTPS</i>	CTP synthase	2.57	1.26E-04
A_24_P174924	NM_003537	<i>HIST1H3B</i>	Histone cluster 1, H3b	2.57	1.26E-04
A_23_P155989	NM_022145	<i>CENPK</i>	Centromere protein K	2.57	1.26E-04
A_23_P103981	NM_001040874	<i>HIST2H2AA4</i>	Histone cluster 2, H2aa4	2.56	1.26E-04
A_23_P571	NM_006516	<i>SLC2A1</i>	Solute carrier family 2 (facilitated glucose transporter), member 1	2.56	1.26E-04
A_23_P420551	NM_007174	<i>CIT</i>	Citron (rho-interacting, serine/threonine kinase 21)	2.56	1.26E-04
A_23_P411335	NM_152524	<i>SGOL2</i>	Shugoshin-like 2 (<i>S. pombe</i>)	2.54	1.26E-04
A_32_P147090	NM_199357	<i>ARHGAP11A</i>	Rho GTPase activating protein 11A	2.54	1.26E-04
A_23_P70448	NM_005325	<i>HIST1H1A</i>	Hstone cluster 1, H1a	2.53	1.26E-04
A_23_P43484	NM_058197	<i>CDKN2A</i>	Cyclin-dependent kinase inhibitor 2A (melanoma, p16, inhibits CDK4)	2.52	1.26E-04
A_24_P85539	NM_212482	<i>FNI</i>	Fibronectin 1	2.52	1.26E-04
A_32_P28704	N/A	N/A		2.52	1.26E-04
A_23_P107421	NM_003258	<i>TK1</i>	Thymidine kinase 1, soluble	2.51	1.26E-04
A_23_P502425	NM_020409	<i>MRPL47</i>	Mitochondrial ribosomal protein L47	2.5	1.26E-04

Table II. Continued.

Probe ID	Accession no.	Symbol	Gene name	Fold change (log)	P-value
A_24_P351466	NM_020890	<i>KIAA1524</i>	KIAA1524	2.5	1.26E-04
A_23_P211910	NM_182943	<i>PLOD2</i>	Procollagen-lysine, 2-oxoglutarate 5-dioxygenase 2	2.5	1.26E-04
A_24_P9321	NM_003533	<i>HIST1H3I</i>	Histone cluster 1, H3i	2.49	1.26E-04
A_24_P334248	NM_014996	<i>PLCH1</i>	Phospholipase C, eta 1	2.48	1.26E-04
A_24_P819890	NM_001005210	<i>LRRC55</i>	Leucine rich repeat containing 55	2.48	4.43E-04
A_23_P146456	NM_001333	<i>CTSL2</i>	Cathepsin L2	2.48	2.33E-04
A_24_P242440	NM_003780	<i>B4GALT2</i>	UDP-Gal:βGlcNAc β 1,4-galactosyltransferase, polypeptide 2	2.47	1.26E-04
A_23_P88331	NM_014750	<i>DLGAP5</i>	Discs, large (<i>Drosophila</i>) homolog-associated protein 5	2.47	1.26E-04
A_23_P216068	NM_014109	<i>ATAD2</i>	ATPase family, AAA domain containing 2	2.46	1.26E-04
A_32_P31021	N/A	N/A		2.46	1.26E-04
A_23_P373119	NR_002165	<i>HMGB3L1</i>	High-mobility group box 3-like 1	2.46	1.26E-04
A_23_P361419	NM_018369	<i>DEPDC1B</i>	DEP domain containing 1B	2.45	1.26E-04
A_23_P10870	NM_014908	<i>DOLK</i>	Dolichol kinase	2.44	1.26E-04
A_23_P420692	NM_015053	<i>PPFIA4</i>	Protein tyrosine phosphatase, receptor type, f polypeptide (PTPRF), interacting protein (liprin), α4	2.43	1.26E-04
A_23_P146284	NM_003129	<i>SQLE</i>	Squalene epoxidase	2.43	1.26E-04
A_32_P159254	AK123584	N/A		2.43	2.33E-04
A_23_P25626	NM_024808	<i>C13orf34</i>	Chromosome 13 open reading frame 34	2.43	1.26E-04
A_23_P59005	NM_000593	<i>TAP1</i>	Transporter 1, ATP-binding cassette, sub-family B (MDR/TAP)	2.43	2.33E-04
A_24_P49747	XM_929965	<i>LOC646993</i>	Similar to high mobility group box 3	2.43	1.26E-04
A_23_P252740	NM_024094	<i>DSCC1</i>	Defective in sister chromatid cohesion 1 homolog (<i>S. cerevisiae</i>)	2.42	1.26E-04
A_23_P397341	NM_152341	<i>PAQR4</i>	Progesterin and adipoQ receptor family member IV	2.42	1.26E-04
A_23_P59045	NM_021052	<i>HIST1H2AE</i>	Histone cluster 1, H2ae	2.42	1.26E-04
A_23_P140316	NM_001099652	<i>GPR137C</i>	G protein-coupled receptor 137C	2.42	1.26E-04
A_23_P207520	Z74615	<i>COL1A1</i>	Collagen, type I, α1	2.41	1.26E-04
A_24_P920968	NM_182625	<i>GEN1</i>	Gen homolog 1, endonuclease (<i>Drosophila</i>)	2.41	1.26E-04
A_23_P366216	NM_003524	<i>HIST1H2BH</i>	Histone cluster 1, H2bh	2.41	1.26E-04
A_23_P217049	NM_014286	<i>FREQ</i>	Frequenin homolog (<i>Drosophila</i>)	2.41	2.33E-04
A_32_P194264	NM_001008708	<i>CHAC2</i>	ChaC, cation transport regulator homolog 2 (<i>E. coli</i>)	2.4	2.33E-04
A_32_P35839	N/A	N/A		2.4	1.26E-04
A_23_P154894	NM_000100	<i>CSTB</i>	Cystatin B (stefin B)	2.4	1.26E-04
A_24_P340066	NM_001421	<i>ELF4</i>	E74-like factor 4 (ets domain transcription factor)	2.4	1.26E-04
A_24_P857404	NM_001093725	<i>MEX3A</i>	mex-3 homolog A (<i>C. elegans</i>)	2.4	1.26E-04
A_24_P133488	NM_017955	<i>CDCA4</i>	Cell division cycle associated 4	2.4	1.26E-04
A_23_P339240	NM_014996	<i>PLCH1</i>	Phospholipase C, eta 1	2.39	2.33E-04
A_23_P52410	NM_145307	<i>RTKN2</i>	Rhotekin 2	2.39	1.26E-04
A_23_P59877	NM_001444	<i>FABP5</i>	Fatty acid binding protein 5 (psoriasis-associated)	2.39	1.26E-04
A_23_P29594	NM_052969	<i>RPL39L</i>	Ribosomal protein L39-like	2.38	1.26E-04
A_23_P11984	NM_201649	<i>SLC6A9</i>	Solute carrier family 6 (neurotransmitter transporter, glycine), member 9	2.38	2.33E-04
A_23_P200866	NM_203401	<i>STMN1</i>	Stathmin 1	2.37	1.26E-04

Table II. Continued.

Probe ID	Accession no.	Symbol	Gene name	Fold change (log)	P-value
A_32_P182135	N/A	N/A		2.36	1.26E-04
A_24_P323598	NM_001017420	<i>ESCO2</i>	Establishment of cohesion 1 homolog 2 (<i>S. cerevisiae</i>)	2.36	1.26E-04
A_23_P39574	NM_001080539	<i>CCDC150</i>	Coiled-coil domain containing 150	2.36	1.26E-04
A_24_P275386	AK025766	<i>BRI3BP</i>	BRI3 binding protein	2.36	1.26E-04
A_23_P85460	NM_078626	<i>CDKN2C</i>	Cyclin-dependent kinase inhibitor 2C (p18, inhibits CDK4)	2.35	1.26E-04
A_23_P57306	NM_005441	<i>CHAF1B</i>	Chromatin assembly factor 1, subunit B (p60)	2.35	1.26E-04
A_23_P335329	NM_004485	<i>GNG4</i>	Guanine nucleotide binding protein (G protein), $\gamma 4$	2.35	2.33E-04
A_23_P92441	NM_002358	<i>MAD2L1</i>	MAD2 mitotic arrest deficient-like 1 (yeast)	2.35	1.26E-04
A_24_P13390	NM_032814	<i>RNFT2</i>	Ring finger protein, transmembrane 2	2.35	1.26E-04
A_23_P362046	NM_138779	<i>C13orf27</i>	Chromosome 13 open reading frame 27	2.34	1.26E-04
A_23_P24716	NM_017870	<i>TMEM132A</i>	Transmembrane protein 132A	2.34	1.26E-04
A_23_P91900	NM_005496	<i>SMC4</i>	structural maintenance of chromosomes 4	2.33	1.26E-04
A_24_P105102	NM_182687	<i>PKMYT1</i>	Protein kinase, membrane associated tyrosine/threonine 1	2.33	1.26E-04
A_24_P244420	NM_018367	<i>ACER3</i>	alkaline ceramidase 3	2.33	2.33E-04
A_23_P112673	NM_017975	<i>ZWILCH</i>	Zwilch, kinetochore associated, homolog (<i>Drosophila</i>)	2.33	1.26E-04
A_23_P87769	NM_017915	<i>C12orf48</i>	Chromosome 12 open reading frame 48	2.33	1.26E-04
A_24_P296254	NM_014783	<i>ARHGAP11A</i>	Rho GTPase activating protein 11A	2.32	1.26E-04
A_23_P166306	NM_000071	<i>CBS</i>	Cystathionine- β -synthase	2.32	1.26E-04

N/A, not annotated; P-value, Benjamini-Hochberg false discovery rate of random permutation test; log fold change, between groups. Gene symbol, accession number and gene name were exported from GeneSpring (from the NCBI databases).

regulated genes in TNBC (cluster 2; enrichment score, 6.43). As shown in Table V and Fig. 2, cluster 2 consisted of functions induced by extracellular matrix-cell adhesion-associated genes such as latent transforming growth factor β binding protein 2 (*LTBP2*), laminin $\alpha 3$ (*LAMA3*) and cell adhesion molecule with homology to L1CAM (close homolog of L1) (*CHL1*), which have been reported to be downregulated in various tumors (35-37). These results suggest that loss of cell-cell or matrix-cell interactions might be a key mechanism in TNBC progression.

Identification of *ASPM* and *CENPK* as novel molecular targets for TNBC therapy. Because the upregulated genes were mainly included in the cell cycle-associated gene cluster as described above, we directed our focus to two cancer-specific genes that function as cell cycle regulators, asp (abnormal spindle) homolog, microcephaly associated (*Drosophila*) (*ASPM*), which is fundamental for cytokinesis (38) and centromere protein K (*CENPK*), which is essential for proper kinetochore assembly during mitosis (39), as novel therapeutic targets for TNBC. qRT-PCR experiments confirmed that *ASPM* and *CENPK* genes were significantly upregulated in 48 clinical TNBC cases (Fig. 3A) and five cell lines derived

from TNBC (Fig. 3B), but undetectably expressed in a mixture of 13 microdissected normal mammary ductal cells and the normal mammary epithelial cell line MCF10A as well as normal human vital organs.

To ascertain the possible roles of *ASPM* and *CENPK* in TNBC cell growth, we knocked down the expression of endogenous *ASPM* and *CENPK* in three TNBC cell lines, HCC1937, BT-20 and MDA-MB-231 cells, which highly express both of these genes (Fig. 3), using RNAi. qRT-PCR experiments showed that *ASPM* and *CENPK* were significantly knocked down in cells transfected with si*ASPM* and si*CENPK*, but not with si*EGFP* as a control (Fig. 4A). In concordance with their knockdown, the MTT assay clearly revealed growth suppression of breast cancer cells in a time-dependent manner by si*ASPM* and si*CENPK*, compared with a control si*EGFP*, which showed no knockdown (Fig. 4B). In addition, a colony formation assay also confirmed that introducing both shRNA-*ASPM* and -*CENPK* constructs remarkably suppressed the growth of BT-20 and MDA-MB-231 cells, respectively, compared with sh*EGFP*-transfected cells (Fig. 4C), suggesting that both genes are likely indispensable for breast cancer cell growth. Furthermore, we investigated the phenotypic alterations of TNBC cells transfected with *ASPM* and *CENPK* siRNAs

Table III. Significantly downregulated genes in TNBC compared with normal ductal cells.

Probe ID	Accession no.	Symbol	Gene name	Fold change (log)	P-value
A_23_P127781	NM_006552	<i>SCGB1D1</i>	Secretoglobin, family 1D, member 1	-6.77	1.26E-04
A_32_P234405	CK570316	N/A		-6.62	1.26E-04
A_23_P150555	NM_006551	<i>SCGB1D2</i>	Secretoglobin, family 1D, member 2	-6.51	1.26E-04
A_23_P12533	NM_052997	<i>ANKRD30A</i>	Ankyrin repeat domain 30A	-6.44	1.26E-04
A_23_P8702	NM_002652	<i>PIP</i>	Prolactin-induced protein	-6.34	1.26E-04
A_23_P501010	NM_000494	<i>COL17A1</i>	Collagen, type XVII, α 1	-5.69	1.26E-04
A_24_P844984	NM_002644	<i>PIGR</i>	Polymeric immunoglobulin receptor	-5.55	1.26E-04
A_32_P216520	NM_007191	<i>WIF1</i>	WNT inhibitory factor 1	-5.53	1.26E-04
A_23_P71364	NM_015886	<i>PII5</i>	Peptidase inhibitor 15	-5.33	1.26E-04
A_24_P273756	NM_003722	<i>TP63</i>	Tumor protein p63	-5.11	1.26E-04
A_23_P132619	NM_000916	<i>OXTR</i>	Oxytocin receptor	-4.89	1.26E-04
A_32_P111873	BQ432543	N/A		-4.88	1.26E-04
A_32_P23272	N/A	N/A		-4.85	1.26E-04
A_24_P643776	N/A	N/A		-4.74	1.26E-04
A_23_P136777	NM_001647	<i>APOD</i>	Apolipoprotein D	-4.71	1.26E-04
A_23_P9711	NM_006040	<i>HS3ST4</i>	Heparan sulfate (glucosamine) 3-O-sulfotransferase 4	-4.58	1.26E-04
A_23_P305292	NR_027180	<i>LOC728264</i>	Hypothetical LOC728264	-4.57	1.26E-04
A_23_P159974	NM_033495	<i>KLHL13</i>	Kelch-like 13 (<i>Drosophila</i>)	-4.55	1.26E-04
A_23_P105144	NM_020974	<i>SCUBE2</i>	Signal peptide, CUB domain, EGF-like 2	-4.51	1.26E-04
A_32_P14253	N/A	N/A		-4.47	1.26E-04
A_23_P327380	NM_003722	<i>TP63</i>	Tumor protein p63	-4.45	1.26E-04
A_23_P337270	AK057247	N/A		-4.43	1.26E-04
A_23_P420442	NM_153618	<i>SEMA6D</i>	Sema domain, transmembrane domain (TM), and cytoplasmic domain, (semaphorin) 6D	-4.34	1.26E-04
A_23_P8812	N/A	N/A		-4.3	1.26E-04
A_23_P160377	NM_003462	<i>DNALII</i>	Dynein, axonemal, light intermediate chain 1	-4.26	1.26E-04
A_24_P92680	AK093340	<i>LOC100132116</i>	Hypothetical LOC100132116	-4.23	1.26E-04
A_23_P216779	NM_001007097	<i>NTRK2</i>	Neurotrophic tyrosine kinase, receptor, type 2	-4.23	1.26E-04
A_23_P148249	NM_024817	<i>THSD4</i>	Thrombospondin, type I, domain containing 4	-4.18	1.26E-04
A_23_P206920	NM_001040114	<i>MYH11</i>	Myosin, heavy chain 11, smooth muscle	-4.13	1.26E-04
A_32_P154473	NM_004522	<i>KIF5C</i>	Kinesin family member 5C	-4.13	1.26E-04
A_23_P128362	NM_206819	<i>MYBPC1</i>	Myosin binding protein C, slow type	-4.11	3.41E-04
A_23_P83381	NM_001143962	<i>CAPN8</i>	Calpain 8	-4.08	1.26E-04
A_23_P397208	NM_000848	<i>GSTM2</i>	Glutathione S-transferase mu 2 (muscle)	-4.07	1.26E-04
A_23_P503072	NM_148672	<i>CCL28</i>	Chemokine (C-C motif) ligand 28	-4.03	1.26E-04
A_23_P143068	NM_024726	<i>IQCA1</i>	IQ motif containing with AAA domain 1	-4.01	1.26E-04
A_24_P829209	AK096334	<i>LOC285944</i>	Hypothetical protein LOC285944	-3.99	2.33E-04
A_23_P394246		<i>GPR81</i>	G protein-coupled receptor 81	-3.96	1.26E-04
A_24_P34186	NM_004010	<i>DMD</i>	Dystrophin	-3.96	1.26E-04
A_23_P303087	NM_002825	<i>PTN</i>	Pleiotrophin	-3.95	1.26E-04
A_24_P243749	NM_002612	<i>PDK4</i>	Pyruvate dehydrogenase kinase, isozyme 4	-3.94	1.26E-04

Table III. Continued.

Probe ID	Accession no.	Symbol	Gene name	Fold change (log)	P-value
A_32_P39944	AK095791	N/A		-3.82	1.26E-04
A_23_P217379	NM_033641	<i>COL4A6</i>	Collagen, type IV, $\alpha 6$	-3.8	1.26E-04
A_23_P407565	NM_001337	<i>CX3CR1</i>	Chemokine (C-X3-C motif) receptor 1	-3.76	1.26E-04
A_23_P373464	NM_002285	<i>AFF3</i>	AF4/FMR2 family, member 3	-3.75	1.26E-04
A_32_P183765	NM_005235	<i>ERBB4</i>	v-erb-a erythroblastic leukemia viral oncogene homolog 4 (avian)	-3.75	1.26E-04
A_23_P145514	NM_014432	<i>IL20RA</i>	Interleukin 20 receptor, α	-3.75	1.26E-04
A_24_P870620	NM_002825	<i>PTN</i>	Pleiotrophin	-3.74	2.33E-04
A_32_P154361	N/A	N/A		-3.73	1.26E-04
A_24_P330633	NM_000353	<i>TAT</i>	Tyrosine aminotransferase	-3.72	1.26E-04
A_23_P360777	NM_013960	<i>NRG1</i>	Neuregulin 1	-3.72	1.26E-04
A_23_P253982	NM_002141	<i>HOXA4</i>	Homeobox A4	-3.69	1.26E-04
A_32_P114475	N/A	N/A		-3.68	1.26E-04
A_32_P221774	BX099483	N/A		-3.66	1.26E-04
A_23_P212608	NM_022131	<i>CLSTN2</i>	Calsyntenin 2	-3.66	2.33E-04
A_23_P254165	NM_021785	<i>RAI2</i>	Retinoic acid induced 2	-3.65	1.26E-04
A_24_P794447	NR_024430	<i>LOC399959</i>	Hypothetical LOC399959	-3.64	1.26E-04
A_23_P149517	NM_002644	<i>PIGR</i>	Polymeric immunoglobulin receptor	-3.64	1.26E-04
A_24_P904484	NR_024344	<i>LOC283174</i>	Hypothetical LOC283174	-3.62	1.26E-04
A_32_P194423	N/A	N/A		-3.62	1.26E-04
A_23_P371495	NM_175861	<i>TMTC1</i>	Transmembrane and tetratricopeptide repeat containing 1	-3.6	2.33E-04
A_23_P134162	NM_016356	<i>DCDC2</i>	Doublecortin domain containing 2	-3.58	1.26E-04
A_32_P232455	NM_178840	<i>C1orf64</i>	Chromosome 1 open reading frame 64	-3.58	1.26E-04
A_24_P318160	NM_014903	<i>NAV3</i>	Neuron navigator 3	-3.57	1.26E-04
A_23_P59388	NM_001723	<i>DST</i>	Dystonin	-3.56	1.26E-04
A_23_P399217	NM_153445	<i>OR5P3</i>	Olfactory receptor, family 5, subfamily P, member 3	-3.56	1.26E-04
A_23_P309739	NM_000125	<i>ESR1</i>	Estrogen receptor 1	-3.53	1.26E-04
A_24_P608007	AK022390	N/A		-3.53	1.26E-04
A_23_P501538	NM_153631	<i>HOXA3</i>	Homeobox A3	-3.52	1.26E-04
A_24_P602871	NM_001030060	<i>SAMD5</i>	Sterile α motif domain containing 5	-3.52	1.26E-04
A_23_P136433	N/A	N/A		-3.51	1.26E-04
A_23_P30294	NM_001801	<i>CDO1</i>	Cysteine dioxygenase, type I	-3.48	1.26E-04
A_23_P218928	NM_016613	<i>FAM198B</i>	Family with sequence similarity 198, member B	-3.47	1.26E-04
A_23_P154627	XM_002345419	<i>TSHZ2</i>	Teashirt zinc finger homeobox 2	-3.47	1.26E-04
A_23_P303833	NM_174934	<i>SCN4B</i>	Sodium channel, voltage-gated, type IV, β	-3.45	1.26E-04
A_24_P930088	XM_002342181	<i>LOC100286909</i>	Hypothetical protein LOC100286909	-3.45	1.26E-04
A_32_P81623	AA514833	N/A		-3.42	1.26E-04
A_24_P923028	BC020707	<i>TAT</i>	Tyrosine aminotransferase	-3.41	1.26E-04
A_23_P58869	NR_002932	<i>LOC442245</i>	Glutathione S-transferase mu 2 pseudogene	-3.4	1.26E-04
A_23_P2271	NM_198965	<i>PTH LH</i>	Parathyroid hormone-like hormone	-3.4	1.26E-04
A_32_P43664				-3.39	1.26E-04
A_32_P16007	NM_207355	<i>POTEB</i>	POTE ankyrin domain family, member B	-3.39	1.26E-04
A_23_P94840	NM_130897	<i>DYNLRB2</i>	Dynein, light chain, roadblock-type 2	-3.38	1.26E-04
A_24_P5153	NM_024817	<i>THSD4</i>	Thrombospondin, type I, domain containing 4	-3.38	1.26E-04

Table III. Continued.

Probe ID	Accession no.	Symbol	Gene name	Fold change (log)	P-value
A_32_P223675	N/A	N/A		-3.37	1.26E-04
A_24_P904845	AK095791	N/A		-3.37	1.26E-04
A_23_P403209	N/A	N/A		-3.36	1.26E-04
A_23_P215382	N/A	N/A		-3.35	3.41E-04
A_24_P209710	NM_004816	<i>FAM189A2</i>	Family with sequence similarity 189, member A2	-3.35	1.26E-04
A_23_P167168	NM_144646	<i>IGJ</i>	Immunoglobulin J polypeptide, linker protein for immunoglobulin α and mu polypeptides	-3.34	1.26E-04
A_24_P70183	NM_001040113	<i>MYH11</i>	Myosin, heavy chain 11, smooth muscle	-3.32	1.26E-04
A_23_P216361	NM_021110	<i>COL14A1</i>	collagen, type XIV, α 1	-3.32	1.26E-04
A_23_P113351	NM_004684	<i>SPARCL1</i>	SPARC-like 1 (hevin)	-3.31	1.26E-04
A_32_P17145	N/A	N/A		-3.31	1.26E-04
A_23_P35414	NM_005398	<i>PPP1R3C</i>	Protein phosphatase 1, regulatory (inhibitor) subunit 3C	-3.29	1.26E-04
A_23_P31945	NM_033439	<i>IL33</i>	Interleukin 33	-3.27	1.26E-04
A_23_P204630	NM_021229	<i>NTN4</i>	Netrin 4	-3.26	1.26E-04
A_23_P501831	NM_032385	<i>C5orf4</i>	Chromosome 5 open reading frame 4	-3.26	1.26E-04
A_23_P200015	NM_174858	<i>AK5</i>	Adenylate kinase 5	-3.26	1.26E-04
A_24_P802145	NM_005544	<i>IRS1</i>	Insulin receptor substrate 1	-3.26	1.26E-04
A_24_P251969	NM_000800	<i>FGF1</i>	Fibroblast growth factor 1 (acidic)	-3.24	1.26E-04
A_32_P228618	NM_001003793	<i>RBMS3</i>	RNA binding motif, single stranded interacting protein	-3.23	1.26E-04
A_23_P125233	NM_001299	<i>CNN1</i>	Calponin 1, basic, smooth muscle	-3.22	2.33E-04
A_23_P500998	NM_152739	<i>HOXA9</i>	Homeobox A9	-3.19	2.33E-04
A_23_P83838	NM_004056	<i>CA8</i>	Carbonic anhydrase VIII	-3.19	1.26E-04
A_24_P911950	N/A	N/A		-3.17	1.26E-04
A_23_P159952	NM_018476	<i>BEX1</i>	Brain expressed, X-linked 1	-3.17	1.26E-04
A_23_P45185	NM_004469	<i>FIGF</i>	c-fos induced growth factor (vascular endothelial growth factor D)	-3.16	2.33E-04
A_23_P14083	NM_181847	<i>AMIGO2</i>	Adhesion molecule with Ig-like domain 2	-3.16	1.26E-04
A_24_P920366	N/A	N/A		-3.14	1.26E-04
A_24_P167668	NM_000428	<i>LTBP2</i>	Latent transforming growth factor β binding protein 2	-3.12	1.26E-04
A_32_P161033	BC043411	N/A		-3.11	1.26E-04
A_23_P348159	NM_020388	<i>DST</i>	Dystonin	-3.11	1.26E-04
A_32_P89415	N/A	N/A		-3.1	1.26E-04
A_23_P165778	NM_024101	<i>MLPH</i>	Melanophilin	-3.08	1.26E-04
A_32_P168701	N/A	N/A		-3.07	3.41E-04
A_32_P78491	NM_004956	<i>ETV1</i>	ets variant 1	-3.06	1.26E-04
A_24_P87036	NM_018043	<i>ANO1</i>	Anoctamin 1, calcium activated chloride channel	-3.06	1.26E-04
A_24_P912799	NM_003966	<i>SEMA5A</i>	Sema domain, seven thrombospondin repeats (type 1 and type 1-like), transmembrane domain (TM) and short cytoplasmic domain, (semaphorin) 5A	-3.06	1.26E-04
A_23_P315364	NM_002089	<i>CXCL2</i>	Chemokine (C-X-C motif) ligand 2	-3.05	1.26E-04
A_24_P71341	NM_001461	<i>FMO5</i>	Flavin containing monooxygenase 5	-3.05	2.33E-04
A_32_P199796	NM_004023	<i>DMD</i>	Dystrophin	-3.05	2.33E-04
A_32_P179998	NM_033053	<i>DMRTC1</i>	DMRT-like family C1	-3.04	1.26E-04
A_32_P17984	N/A	N/A		-3.04	1.26E-04

Table III. Continued.

Probe ID	Accession no.	Symbol	Gene name	Fold change (log)	P-value
A_23_P138938	NM_000926	<i>PGR</i>	Progesterone receptor	-3.04	1.26E-04
A_23_P18559	NM_003866	<i>INPP4B</i>	Inositol polyphosphate-4-phosphatase, type II, 105 kDa	-3.03	1.26E-04
A_23_P124946	NM_153610	<i>CMYA5</i>	Cardiomyopathy associated 5	-3.03	1.26E-04
A_23_P212241	NM_006614	<i>CHL1</i>	Cell adhesion molecule with homology to LICAM (close homolog of L1)	-3.03	1.26E-04
A_23_P156402	NM_003551	<i>NME5</i>	Non-metastatic cells 5, protein expressed in (nucleoside-diphosphate kinase)	-3.02	1.26E-04
A_23_P150053	NM_001613	<i>ACTA2</i>	Actin, α 2, smooth muscle, aorta	-3.02	1.26E-04
A_32_P58912	N/A	N/A		-3.02	1.26E-04
A_32_P216841	NM_145263	<i>SPATA18</i>	Spermatogenesis associated 18 homolog (rat)	-3.01	2.33E-04
A_23_P257087	NM_002612	<i>PDK4</i>	Pyruvate dehydrogenase kinase, isozyme 4	-3.01	1.26E-04
A_23_P110686	NM_003714	<i>STC2</i>	Stanniocalcin 2	-3	1.26E-04
A_23_P369994	NM_004734	<i>DCLK1</i>	Doublecortin-like kinase 1	-2.99	2.33E-04
A_23_P422831	NM_004816	<i>FAM189A2</i>	Family with sequence similarity 189, member A2	-2.98	1.26E-04
A_24_P325992	NM_002310	<i>LIFR</i>	Leukemia inhibitory factor receptor α	-2.98	1.26E-04
A_23_P387000	NM_173683	<i>XKR6</i>	XK, Kell blood group complex subunit-related family, member 6	-2.98	3.41E-04
A_32_P83811	NM_001136570	<i>FAM47E</i>	Family with sequence similarity 47, member E	-2.98	1.26E-04
A_32_P44210	BX538299	N/A		-2.97	1.26E-04
A_24_P918317	NM_015881	<i>DKK3</i>	Dickkopf homolog 3 (<i>Xenopus laevis</i>)	-2.97	4.43E-04
A_23_P203957	NM_175861	<i>TMTC1</i>	Transmembrane and tetratricopeptide repeat containing 1	-2.96	3.41E-04
A_23_P30217	NM_052863	<i>SCGB3A1</i>	Secretoglobin, family 3A, member 1	-2.96	1.26E-04
A_23_P77066	NM_022807	<i>SNRPN</i>	Small nuclear ribonucleoprotein polypeptide N	-2.94	1.26E-04
A_32_P109242	AK055302	<i>CSRNP3</i>	Cysteine-serine-rich nuclear protein 3	-2.91	1.26E-04
A_24_P937265	N/A	N/A		-2.91	1.26E-04
A_32_P97968	N/A	N/A		-2.9	1.26E-04
A_32_P85684	AA069768	N/A		-2.89	1.26E-04
A_23_P385067	NM_053277	<i>CLIC6</i>	Chloride intracellular channel 6	-2.89	4.43E-04
A_23_P82868	NM_000930	<i>PLAT</i>	Plasminogen activator, tissue	-2.88	1.26E-04
A_32_P108396	N/A	N/A		-2.88	1.26E-04
A_23_P148345	NM_194463	<i>RNF128</i>	Ring finger protein 128	-2.87	1.26E-04
A_24_P314477	NM_178012	<i>TUBB2B</i>	Tubulin, β 2B	-2.87	1.26E-04
A_24_P895836	N/A	N/A		-2.87	1.26E-04
A_23_P171074	NM_004867	<i>ITM2A</i>	Integral membrane protein 2A	-2.85	1.26E-04
A_23_P9135	NM_033655	<i>CNTNAP3</i>	Contactin associated protein-like 3	-2.85	4.43E-04
A_23_P372234	NM_001218	<i>CA12</i>	Carbonic anhydrase XII	-2.83	1.26E-04
A_23_P393099	NM_003226	<i>TFF3</i>	Trefoil factor 3 (intestinal)	-2.82	2.33E-04
A_23_P113701	NM_002607	<i>PDGFA</i>	Platelet-derived growth factor α polypeptide	-2.82	1.26E-04
A_23_P10995	NM_014483	<i>RBMS3</i>	RNA binding motif, single stranded interacting protein	-2.82	1.26E-04
A_24_P269006	NM_001182	<i>ALDH7A1</i>	Aldehyde dehydrogenase 7 family, member A1	-2.81	1.26E-04
A_23_P415533	AK054879	N/A		-2.81	1.26E-04
A_23_P216225	NM_004430	<i>EGR3</i>	Early growth response 3	-2.8	1.26E-04
A_24_P101282	N/A	N/A		-2.8	1.26E-04
A_32_P72541	N/A	N/A		-2.8	2.33E-04
A_24_P299474	NM_001122679	<i>ODZ2</i>	odz, odd Oz/ten-m homolog 2 (<i>Drosophila</i>)	-2.8	1.26E-04

Table III. Continued.

Probe ID	Accession no.	Symbol	Gene name	Fold change (log)	P-value
A_23_P416395	NM_003714	<i>STC2</i>	Stanniocalcin 2	-2.8	1.26E-04
A_23_P40415	NM_007038	<i>ADAMTS5</i>	ADAM metallopeptidase with thrombospondin type 1 motif, 5	-2.8	1.26E-04
A_32_P3545	XM_002345868	<i>LOC100131504</i>	Hypothetical LOC100131504	-2.79	4.43E-04
A_23_P106405	NM_002487	<i>NDN</i>	Necdin homolog (mouse)	-2.79	1.26E-04
A_23_P405129	NM_000428	<i>LTBP2</i>	Latent transforming growth factor β binding protein 2	-2.79	1.26E-04
A_24_P237804	NM_174981	<i>POTED</i>	POTE ankyrin domain family, member D	-2.78	1.26E-04
A_23_P89780	NM_198129	<i>LAMA3</i>	Laminin, $\alpha 3$	-2.78	1.26E-04
A_23_P213415	NM_003966	<i>SEMA5A</i>	Sema domain, seven thrombospondin repeats (type 1 and type 1-like), transmembrane domain (TM) and short cytoplasmic domain, (semaphorin) 5A	-2.77	3.41E-04
A_24_P397386	NM_002310	<i>LIFR</i>	Leukemia inhibitory factor receptor α	-2.77	1.26E-04
A_23_P73297	NM_004742	<i>MAGII</i>	Membrane associated guanylate kinase, WW and PDZ domain containing 1	-2.77	1.26E-04
A_23_P165783	NM_024101	<i>MLPH</i>	Melanophilin	-2.76	1.26E-04
A_23_P212061	NM_007289	<i>MME</i>	Membrane metallo-endopeptidase	-2.76	1.26E-04
A_23_P75056	NM_001002295	<i>GATA3</i>	GATA binding protein 3	-2.76	1.26E-04
A_24_P748377	CR749529			-2.75	2.33E-04
A_24_P810476		<i>NTRK3</i>	Neurotrophic tyrosine kinase, receptor, type 3	-2.74	3.41E-04
A_32_P60606	AL713753	<i>DKFZp667F0711</i>	Hypothetical protein DKFZp667F0711	-2.74	1.26E-04
A_32_P200697	NM_181709	<i>FAM101A</i>	Family with sequence similarity 101, member A	-2.73	4.43E-04
A_24_P84220	NR_027995	<i>LOC284232</i>	Ankyrin repeat domain 20 family, member A2 pseudogene	-2.73	1.26E-04
A_23_P157914	NM_153267	<i>MAMDC2</i>	MAM domain containing 2	-2.71	1.26E-04
A_24_P393596	N/A	N/A		-2.71	1.26E-04
A_32_P25419	N/A	N/A		-2.7	1.26E-04
A_24_P169873	N/A	N/A		-2.7	1.26E-04
A_24_P358534	N/A	N/A		-2.69	3.41E-04
A_32_P34750	AV702101	N/A		-2.69	1.26E-04
A_32_P9941	NM_007191	<i>WIF1</i>	WNT inhibitory factor 1	-2.68	2.33E-04
A_23_P335143	U81001	<i>SNRPN</i>	Small nuclear ribonucleoprotein polypeptide N	-2.67	1.26E-04
A_23_P56855	NM_001137671	<i>POTEC</i>	POTE ankyrin domain family, member C	-2.67	1.26E-04
A_32_P59837	AK091914	N/A		-2.65	1.26E-04
A_24_P737553	AK023774	N/A		-2.65	2.33E-04
A_23_P204286	NM_000900	<i>MGP</i>	Matrix Gla protein	-2.65	1.26E-04
A_24_P725895	BE218249	N/A		-2.63	1.26E-04
A_32_P4337	N/A	N/A		-2.63	1.26E-04
A_23_P154400	NM_001042467	<i>MLPH</i>	Melanophilin	-2.62	1.26E-04
A_23_P29800	NM_005602	<i>CLDN11</i>	Claudin 11	-2.61	1.26E-04
A_23_P156025	NM_033267	<i>IRX2</i>	Iroquois homeobox 2	-2.61	1.26E-04
A_32_P193091	N/A	N/A		-2.61	1.26E-04
A_23_P83857	NM_000240	<i>MAOA</i>	Monoamine oxidase A	-2.6	1.26E-04
A_32_P355396	NM_014844	<i>TECPR2</i>	Tectonin β -propeller repeat containing 2	-2.6	1.26E-04
A_32_P214565	BU928689	N/A		-2.6	1.26E-04

Table III. Continued.

Probe ID	Accession no.	Symbol	Gene name	Fold change (log)	P-value
A_24_P468950	AK021439	N/A		-2.6	1.26E-04
A_24_P683583	N/A	N/A		-2.6	1.26E-04
A_23_P203558	NM_000518	<i>HBB</i>	Hemoglobin, β	-2.6	2.33E-04
A_32_P140153	N/A	N/A		-2.6	1.26E-04
A_32_P124461	AK129743	N/A		-2.59	1.26E-04
A_23_P136026	AK128476	N/A		-2.59	1.26E-04
A_23_P28295	NM_004525	<i>LRP2</i>	Low density lipoprotein-related protein 2	-2.59	4.43E-04
A_24_P586712	NM_198485	<i>TPRG1</i>	Tumor protein p63 regulated 1	-2.58	1.26E-04
A_23_P139500	NM_030762	<i>BHLHE41</i>	Basic helix-loop-helix family, member e41	-2.58	1.26E-04
A_23_P121480	NM_001004196	<i>CD200</i>	CD200 molecule	-2.58	1.26E-04
A_23_P32577	NM_080759	<i>DACHI</i>	Dachshund homolog 1 (<i>Drosophila</i>)	-2.58	1.26E-04
A_23_P315815	NM_004495	<i>NRG1</i>	Neuregulin 1	-2.58	1.26E-04
A_23_P93772	NM_019102	<i>HOXA5</i>	Homeobox A5	-2.58	1.26E-04
A_32_P150748	CR749529	N/A		-2.58	1.26E-04
A_32_P204959	N/A	N/A		-2.58	1.26E-04
A_23_P363149	N/A	N/A		-2.57	4.43E-04
A_23_P41487	NM_015130	<i>TBC1D9</i>	TBC1 domain family, member 9 (with GRAM domain)	-2.57	1.26E-04
A_23_P257296	NM_003226	<i>TFF3</i>	Trefoil factor 3 (intestinal)	-2.56	3.41E-04
A_23_P250735	NM_175709	<i>CBX7</i>	Chromobox homolog 7	-2.56	1.26E-04
A_24_P189516	NM_001609	<i>ACADSB</i>	acyl-coenzyme A dehydrogenase, short/branched chain	-2.56	1.26E-04
A_23_P253012	NM_017577	GRAMD1C	GRAM domain containing 1C	-2.56	1.26E-04
A_24_P179244	XM_001723863	<i>LOC100128979</i>	Hypothetical protein LOC100128979	-2.55	1.26E-04
A_32_P117846	N/A	N/A		-2.55	1.26E-04
A_32_P42224	BX097190	N/A		-2.55	2.33E-04
A_24_P119665	NM_001128933	<i>SYNPO2</i>	Synaptopodin 2	-2.54	1.26E-04
A_32_P105825	NM_001584	<i>MPPED2</i>	Metallophosphoesterase domain containing 2	-2.54	3.41E-04
A_24_P225679	NM_005544	<i>IRS1</i>	Insulin receptor substrate 1	-2.54	1.26E-04
A_32_P226907	N/A	N/A		-2.54	1.26E-04
A_23_P356581	NM_022370	<i>ROBO3</i>	Roundabout, axon guidance receptor, homolog 3 (<i>Drosophila</i>)	-2.53	1.26E-04
A_32_P221096	AW015426	N/A		-2.53	1.26E-04
A_23_P106016	NM_002742	<i>PRKDI</i>	Protein kinase D1	-2.52	1.26E-04
A_32_P210193	N/A	N/A		-2.52	1.26E-04
A_32_P38436	N/A	N/A		-2.52	1.26E-04
A_24_P512775	N/A	N/A		-2.52	1.26E-04
A_23_P151529	NR_023938	<i>C14orf132</i>	Chromosome 14 open reading frame 132	-2.52	1.26E-04
A_32_P235568	AK125221	N/A		-2.52	1.26E-04
A_23_P71270	NM_001185	<i>AZGP1</i>	α -2-glycoprotein 1, zinc-binding	-2.52	4.43E-04
A_24_P650425	N/A	N/A		-2.51	1.26E-04
A_23_P71328	NM_030583	<i>MATN2</i>	Matrilin 2	-2.51	2.33E-04
A_24_P153803	NM_020663	<i>RHOJ</i>	ras homolog gene family, member J	-2.51	1.26E-04
A_24_P912730	N/A	N/A		-2.51	1.26E-04
A_24_P347624	NM_022804	<i>SNURF</i>	SNRPN upstream reading frame	-2.5	1.26E-04
A_32_P52785	NM_015345	<i>DAAM2</i>	Dishevelled associated activator of morphogenesis 2	-2.5	3.41E-04
A_23_P61042	N/A	N/A		-2.5	1.26E-04

Table III. Continued.

Probe ID	Accession no.	Symbol	Gene name	Fold change (log)	P-value
A_23_P67661	NM_001864	<i>COX7A1</i>	Cytochrome c oxidase subunit VIIa polypeptide 1 (muscle)	-2.49	1.26E-04
A_23_P213486	N/A	<i>PARP8</i>	Poly(ADP-ribose) polymerase family, member 8	-2.49	1.26E-04
A_23_P18713	NM_004827	<i>ABCG2</i>	ATP-binding cassette, sub-family G (WHITE), member 2	-2.48	4.43E-04
A_23_P76658	NM_052818	<i>N4BP2L1</i>	NEDD4 binding protein 2-like 1	-2.48	1.26E-04
A_23_P96590	NM_014710	<i>GPRASP1</i>	G protein-coupled receptor associated sorting protein 1	-2.48	1.26E-04
A_24_P460763	AK022443	N/A		-2.48	1.26E-04
A_23_P85672	NM_006610	<i>MASP2</i>	Mannan-binding lectin serine peptidase 2	-2.48	1.26E-04
A_24_P416489	N/A	N/A		-2.47	1.26E-04
A_24_P321525	NM_032918	<i>RERG</i>	RAS-like, estrogen-regulated, growth inhibitor	-2.47	1.26E-04
A_24_P256526	BC005914	<i>SP2</i>	Sp2 transcription factor	-2.47	1.26E-04
A_24_P261417	NM_015881	<i>DKK3</i>	Dickkopf homolog 3 (<i>Xenopus laevis</i>)	-2.47	1.26E-04
A_23_P98369	NM_000829	<i>GRIA4</i>	Glutamate receptor, ionotropic, AMPA 4	-2.47	1.26E-04
A_23_P6818	NM_020163	<i>SEMA3G</i>	Sema domain, immunoglobulin domain (Ig), short basic domain, secreted, (semaphorin) 3G	-2.46	3.41E-04
A_32_P100379	N/A	N/A		-2.46	1.26E-04
A_23_P30163	NR_026804	<i>FLJ13197</i>	Hypothetical FLJ13197	-2.46	1.26E-04
A_24_P206328	NM_005020	<i>PDE1C</i>	Phosphodiesterase 1C, calmodulin-dependent 70 kDa	-2.46	1.26E-04
A_24_P93948	AB210045	N/A		-2.46	1.26E-04
A_32_P52414	N/A	N/A		-2.45	1.26E-04
A_23_P123228	NM_000111	<i>SLC26A3</i>	Solute carrier family 26, member 3	-2.45	1.26E-04
A_24_P666553	N/A	N/A		-2.45	1.26E-04
A_24_P916816	N/A	N/A		-2.44	1.26E-04
A_23_P134734	NM_017786	<i>GOLSYN</i>	Golgi-localized protein	-2.44	1.26E-04
A_24_P296772	NM_033256	<i>PPP1R14A</i>	Protein phosphatase 1, regulatory (inhibitor) subunit 14A	-2.43	1.26E-04
A_24_P267523	NM_144613	<i>COX6B2</i>	Cytochrome c oxidase subunit VIb polypeptide 2 (testis)	-2.43	1.26E-04
A_23_P133517	NM_002310	<i>LIFR</i>	Leukemia inhibitory factor receptor α	-2.43	1.26E-04
A_24_P787680	N/A	N/A		-2.43	1.26E-04
A_32_P52829	N/A	N/A		-2.43	3.41E-04
A_23_P162047	NM_015881	<i>DKK3</i>	Dickkopf homolog 3 (<i>Xenopus laevis</i>)	-2.43	1.26E-04
A_32_P185140	BX648171	<i>TPM1</i>	Tropomyosin 1 (α)	-2.43	1.26E-04
A_24_P319892	NM_198274	<i>SMYD1</i>	SET and MYND domain containing 1	-2.43	1.26E-04
A_24_P226322	NM_031469	<i>SH3BGRL2</i>	SH3 domain binding glutamic acid-rich protein like 2	-2.42	1.26E-04
A_23_P86012	NM_001017402	<i>LAMB3</i>	Laminin, β 3	-2.42	1.26E-04
A_23_P62255	NM_005314	<i>GRPR</i>	Gastrin-releasing peptide receptor	-2.41	1.26E-04
A_24_P141520	N/A	N/A		-2.41	2.33E-04
A_23_P114883	NM_002023	<i>FMOD</i>	Fibromodulin	-2.41	1.26E-04
A_23_P300033	NM_006206	<i>PDGFRA</i>	Platelet-derived growth factor receptor, α polypeptide	-2.41	2.33E-04
A_24_P108311	NM_015277	<i>NEDD4L</i>	Neural precursor cell expressed, developmentally downregulated 4-like	-2.41	1.26E-04

Table III. Continued.

Probe ID	Accession no.	Symbol	Gene name	Fold change (log)	P-value
A_23_P345746	NM_199261	<i>TPTE</i>	Transmembrane phosphatase with tensin homology	-2.41	1.26E-04
A_23_P418083	NM_181714	<i>LCA5</i>	Leber congenital amaurosis 5	-2.41	1.26E-04
A_32_P208341	N/A	N/A		-2.41	1.26E-04
A_24_P930337	N/A	N/A		-2.41	1.26E-04
A_24_P915095	NM_017577	<i>GRAMD1C</i>	GRAM domain containing 1C	-2.4	1.26E-04
A_32_P4792	AK057820	N/A		-2.4	1.26E-04
A_24_P82032	NM_020663	<i>RHOJ</i>	ras homolog gene family, member J	-2.39	2.33E-04
A_23_P204296	NM_032918	<i>RERG</i>	RAS-like, estrogen-regulated, growth inhibitor	-2.38	1.26E-04
A_24_P920712	N/A	N/A		-2.38	2.33E-04
A_24_P401185	NM_001042784	<i>CCDC158</i>	Coiled-coil domain containing 158	-2.38	1.26E-04
A_32_P109604	XM_001715342	<i>LOC100132733</i>	Similar to FLJ00310 protein	-2.37	1.26E-04
A_24_P131173	NM_024709	<i>C1orf115</i>	Chromosome 1 open reading frame 115	-2.37	2.33E-04
A_24_P64241	NM_001012421	<i>ANKRD20A2</i>	Ankyrin repeat domain 20 family, member A2	-2.37	1.26E-04
A_32_P58437	N/A	N/A		-2.37	1.26E-04
A_24_P602348	N/A	N/A		-2.37	1.26E-04
A_24_P135856	NM_016124	<i>RHD</i>	Rh blood group, D antigen	-2.37	1.26E-04
A_23_P333038	NM_025145	<i>C10orf79</i>	Chromosome 10 open reading frame 79	-2.37	2.33E-04
A_23_P352266	NM_000633	<i>BCL2</i>	B-cell CLL/lymphoma 2	-2.36	1.26E-04
A_23_P207699	NM_016835	<i>MAPT</i>	Microtubule-associated protein tau	-2.36	1.26E-04
A_23_P392529	NR_027270	<i>C21orf81</i>	Ankyrin repeat domain 20 family, member A3 pseudogene	-2.36	1.26E-04
A_23_P904	NM_024603	<i>BEND5</i>	BEN domain containing 5	-2.36	1.26E-04
A_23_P115785	NM_145235	<i>FANK1</i>	Fibronectin type III and ankyrin repeat domains 1	-2.35	1.26E-04
A_32_P146844	N/A	N/A		-2.35	1.26E-04
A_23_P26865	NM_002470	<i>MYH3</i>	Myosin, heavy chain 3, skeletal muscle, embryonic	-2.35	1.26E-04
A_32_P100641	XM_001714998	<i>LOC100128139</i>	Hypothetical LOC100128139	-2.35	2.33E-04
A_24_P930727	AK091677	N/A		-2.35	1.26E-04
A_23_P406341	NM_001001936	<i>AFAP1L2</i>	Actin filament associated protein 1-like 2	-2.35	1.26E-04
A_24_P54863	NM_152400	<i>C4orf32</i>	Chromosome 4 open reading frame 32	-2.34	1.26E-04
A_23_P133120	NM_018342	<i>TMEM144</i>	Transmembrane protein 144	-2.34	1.26E-04
A_32_P86705	BC040577	N/A		-2.34	1.26E-04
A_24_P833256	N/A	N/A		-2.33	1.26E-04
A_23_P401106	NM_002599	<i>PDE2A</i>	Phosphodiesterase 2A, cGMP-stimulated	-2.33	1.26E-04
A_24_P102119	AF264623	N/A		-2.33	1.26E-04
A_23_P358714	NM_020775	<i>KIAA1324</i>	KIAA1324	-2.32	1.26E-04
A_32_P162494	N/A	N/A		-2.32	3.41E-04
A_23_P326931	NM_145170	<i>TTC18</i>	Tetratricopeptide repeat domain 18	-2.32	1.26E-04

N/A, not annotated; P-value, Benjamini-Hochberg false discovery rate of random permutation test; log fold change, between groups. Gene symbol, accession number and gene name were exported from GeneSpring (from the NCBI databases).

showing significant knockdown effects. FACS analysis revealed that depleting *ASPM* caused a cell cycle arrest at the G2/M phase in HCC1937 cells (siEGFP:siASPM, 24.4:34.0%) at 2 days after transfection, and a subsequent increase in the

Table IV. Genes specifically expressed in TNBC, but not expressed in normal human vital organs.

Probe ID	Accession no.	Symbol	Gene name	Fold change (log)	P-value
A_23_P118834	NM_001067	<i>TOP2A</i>	Topoisomerase (DNA) II α 170 kDa	4.76	1.26E-04
A_32_P119154	BE138567	N/A		4.75	1.26E-04
A_23_P35219	NM_002497	<i>NEK2</i>	NIMA (never in mitosis gene a)-related kinase 2	4.67	1.26E-04
A_23_P166360	NM_206956	<i>PRAME</i>	Preferentially expressed antigen in melanoma	4.64	1.26E-04
A_24_P332314	NM_198947	<i>FAM111B</i>	Family with sequence similarity 111, member B	4.63	1.26E-04
A_24_P413884	NM_001809	<i>CENPA</i>	Centromere protein A	4.59	1.26E-04
A_23_P68610	NM_012112	<i>TPX2</i>	TPX2, microtubule-associated, homolog (Xenopus laevis)	4.58	1.26E-04
A_23_P401	NM_016343	<i>CENPF</i>	Centromere protein F, 350/400 ka (mitosin)	4.44	1.26E-04
A_23_P57379	NM_003504	<i>CDC45L</i>	CDC45 cell division cycle 45-like (<i>S. cerevisiae</i>)	4.44	1.26E-04
A_23_P356684	NM_018685	<i>ANLN</i>	Anillin, actin binding protein	4.29	1.26E-04
A_23_P52017	NM_018136	<i>ASPM</i>	asp (abnormal spindle) homolog, microcephaly associated (<i>Drosophila</i>)	4.17	1.26E-04
A_32_P199884	NM_032132	<i>HORMAD1</i>	HORMA domain containing 1	4.13	2.33E-04
A_23_P259586	NM_003318	<i>TTK</i>	TTK protein kinase	4.09	1.26E-04
A_23_P200310	NM_017779	<i>DEPDC1</i>	DEP domain containing 1	4.08	1.26E-04
A_23_P115872	NM_018131	<i>CEP55</i>	Centrosomal protein 55 kDa	4.03	1.26E-04
A_24_P911179	NM_018136	<i>ASPM</i>	asp (abnormal spindle) homolog, microcephaly associated (<i>Drosophila</i>)	4.02	1.26E-04
A_24_P96780	NM_016343	<i>CENPF</i>	Centromere protein F, 350/400 ka (mitosin)	3.92	1.26E-04
A_24_P14156	NM_006101	<i>NDC80</i>	NDC80 homolog, kinetochore complex component (<i>S. cerevisiae</i>)	3.86	1.26E-04
A_23_P254733	NM_024629	<i>MLF1IP</i>	MLF1 interacting protein	3.85	1.26E-04
A_23_P74115	NM_003579	<i>RAD54L</i>	RAD54-like (<i>S. cerevisiae</i>)	3.84	1.26E-04
A_23_P50108	NM_006101	<i>NDC80</i>	NDC80 homolog, kinetochore complex component (<i>S. cerevisiae</i>)	3.84	1.26E-04
A_23_P155815	NM_022346	<i>NCAPG</i>	Non-SMC condensin I complex, subunit G	3.82	1.26E-04
A_23_P51085	NM_020675	<i>SPC25</i>	SPC25, NDC80 kinetochore complex component, homolog (<i>S. cerevisiae</i>)	3.81	1.26E-04
A_32_P62997	NM_018492	<i>PBK</i>	PDZ binding kinase	3.8	1.26E-04
A_23_P256956	NM_005733	<i>KIF20A</i>	Kinesin family member 20A	3.79	1.26E-04
A_23_P212844	NM_006342	<i>TACC3</i>	Transforming, acidic coiled-coil containing protein 3	3.78	1.26E-04
A_24_P254705	NM_020394	<i>ZNF695</i>	Zinc finger protein 695	3.76	1.26E-04
A_23_P432352	NM_001017978	<i>CXorf61</i>	Chromosome X open reading frame 61	3.73	1.26E-04
A_23_P48669	NM_005192	<i>CDKN3</i>	Cyclin-dependent kinase inhibitor 3	3.71	1.26E-04
A_23_P94571	NM_004432	<i>ELAVL2</i>	ELAV (embryonic lethal, abnormal vision, <i>Drosophila</i>)-like 2 (Hu antigen B)	3.67	1.26E-04
A_23_P150667	NM_031217	<i>KIF18A</i>	Kinesin family member 18A	3.64	1.26E-04
A_32_P68525	BC035392	N/A		3.58	1.26E-04
A_24_P319613	NM_002497	<i>NEK2</i>	NIMA (never in mitosis gene a)-related kinase 2	3.53	1.26E-04
A_23_P10385	NM_016448	<i>DTL</i>	Denticleless homolog (<i>Drosophila</i>)	3.53	1.26E-04
A_23_P94422	NM_014791	<i>MELK</i>	Maternal embryonic leucine zipper kinase	3.5	1.26E-04
A_23_P340909	BC013418	<i>SKA3</i>	Spindle and kinetochore associated complex subunit 3	3.48	1.26E-04
A_23_P124417	NM_004336	<i>BUB1</i>	Budding uninhibited by benzimidazoles 1 homolog (yeast)	3.47	1.26E-04
A_24_P257099	NM_018410	<i>HJURP</i>	Holliday junction recognition protein	3.43	1.26E-04

Table IV. Continued.

Probe ID	Accession no.	Symbol	Gene name	Fold change (log)	P-value
A_23_P74349	NM_145697	<i>NUF2</i>	NUF2, NDC80 kinetochore complex component, homolog (<i>S. cerevisiae</i>)	3.36	1.26E-04
A_24_P302584	NM_003108	<i>SOX11</i>	SRY (sex determining region Y)-box 11	3.36	4.43E-04
A_24_P68088	NR_002947	<i>TCAM1</i>	Testicular cell adhesion molecule 1 homolog (mouse)	3.35	2.33E-04
A_24_P366033	NM_018098	<i>ECT2</i>	Epithelial cell transforming sequence 2 oncogene	3.34	1.26E-04
A_23_P93258	NM_003537	<i>HIST1H3B</i>	Histone cluster 1, H3b	3.33	1.26E-04
A_23_P149668	NM_014875	<i>KIF14</i>	Kinesin family member 14	3.29	1.26E-04
A_23_P34325	NM_033300	<i>LRP8</i>	Low density lipoprotein receptor-related protein 8, apolipoprotein E receptor	3.28	1.26E-04
A_32_P56154	N/A	N/A		3.28	1.26E-04
A_23_P138507	NM_001786	<i>CDC2</i>	Cell division cycle 2, G1→S and G2→M	3.24	1.26E-04
A_23_P49972	NM_001254	<i>CDC6</i>	Cell division cycle 6 homolog (<i>S. cerevisiae</i>)	3.22	1.26E-04
A_24_P306896	XR_040656	<i>LOC283711</i>	Hypothetical protein LOC283711	3.22	1.26E-04
A_23_P44684	NM_018098	<i>ECT2</i>	Epithelial cell transforming sequence 2 oncogene	3.21	1.26E-04
A_23_P100344	NM_014321	<i>ORC6L</i>	Origin recognition complex, subunit 6 like (yeast)	3.2	1.26E-04
A_23_P163481	NM_001211	<i>BUB1B</i>	Budding uninhibited by benzimidazoles 1 homolog β (yeast)	3.17	1.26E-04
A_32_P87849	N/A	N/A		3.16	1.26E-04
A_24_P397107	NM_001789	<i>CDC25A</i>	Cell division cycle 25 homolog A (<i>S. pombe</i>)	3.15	1.26E-04
A_23_P209200	NM_001238	<i>CCNE1</i>	Cyclin E1	3.15	1.26E-04
A_32_P16625	N/A	N/A		3.15	1.26E-04
A_24_P37903	N/A	<i>LOX</i>	Lysyl oxidase	3.12	1.26E-04
A_24_P313504	NM_005030	<i>PLK1</i>	Polo-like kinase 1 (<i>Drosophila</i>)	3.07	1.26E-04
A_23_P252292	NM_006733	<i>CENPI</i>	Centromere protein I	3.04	1.26E-04
A_23_P161474	NM_182751	<i>MCM10</i>	Minichromosome maintenance complex component 10	2.99	1.26E-04
A_23_P253762	N/A	N/A		2.94	1.26E-04
A_24_P225534	NM_017821	<i>RHBDL2</i>	Rhomboid, veinlet-like 2 (<i>Drosophila</i>)	2.94	1.26E-04
A_24_P412088	NM_182751	<i>MCM10</i>	Minichromosome maintenance complex component 10	2.94	1.26E-04
A_32_P109296	NM_152259	<i>C15orf42</i>	Chromosome 15 open reading frame 42	2.91	1.26E-04
A_24_P76521	AK056691	<i>GSG2</i>	Germ cell associated 2 (haspin)	2.83	1.26E-04
A_23_P126212	NM_022111	<i>CLSPN</i>	Claspin homolog (<i>Xenopus laevis</i>)	2.83	1.26E-04
A_23_P60120	NM_031415	<i>GSDMC</i>	Gasdermin C	2.81	2.33E-04
A_24_P902509	NM_018193	<i>FANCI</i>	Fanconi anemia, complementation group I	2.8	1.26E-04
A_23_P155969	NM_014264	<i>PLK4</i>	Polo-like kinase 4 (<i>Drosophila</i>)	2.79	1.26E-04
A_32_P183218	NM_153695	<i>ZNF367</i>	Zinc finger protein 367	2.77	1.26E-04
A_23_P46118	NM_001821	<i>CHML</i>	Choroideremia-like (Rab escort protein 2)	2.76	2.33E-04
A_23_P327643	N/A	N/A		2.75	1.26E-04
A_23_P215976	NM_057749	<i>CCNE2</i>	Cyclin E2	2.72	2.33E-04
A_32_P151800	NM_207418	<i>FAM72D</i>	Family with sequence similarity 72, member D	2.7	1.26E-04
A_23_P34788	NM_006845	<i>KIF2C</i>	Kinesin family member 2C	2.7	1.26E-04
A_23_P133956	NM_002263	<i>KIFC1</i>	Kinesin family member C1	2.69	1.26E-04
A_23_P88630	NM_000057	<i>BLM</i>	Bloom syndrome, RecQ helicase-like	2.68	1.26E-04
A_24_P276102	NM_183404	<i>RBL1</i>	Retinoblastoma-like 1 (p107)	2.68	1.26E-04
A_23_P23303	NM_003686	<i>EXO1</i>	Exonuclease 1	2.67	1.26E-04
A_23_P88691	NM_000745	<i>CHRNA5</i>	Cholinergic receptor, nicotinic, α5	2.67	1.26E-04
A_32_P72341	NM_173084	<i>TRIM59</i>	Tripartite motif-containing 59	2.62	1.26E-04

Table IV. Continued.

Probe ID	Accession no.	Symbol	Gene name	Fold change (log)	P-value
A_24_P227091	NM_004523	<i>KIF11</i>	Kinesin family member 11	2.61	1.26E-04
A_23_P136805	NM_014783	<i>ARHGAP11A</i>	Rho GTPase activating protein 11A	2.6	1.26E-04
A_23_P63402	NM_013296	<i>GPSM2</i>	G-protein signaling modulator 2 (AGS3-like, <i>C. elegans</i>)	2.6	1.26E-04
A_23_P35871	NM_024680	<i>E2F8</i>	E2F transcription factor 8	2.58	1.26E-04
A_23_P207307	N/A	N/A		2.58	1.26E-04
A_24_P399888	NM_001002876	<i>CENPM</i>	Centromere protein M	2.58	1.26E-04
A_23_P155989	NM_022145	<i>CENPK</i>	Centromere protein K	2.57	1.26E-04
A_23_P411335	NM_152524	<i>SGOL2</i>	Shugoshin-like 2 (<i>S. pombe</i>)	2.54	1.26E-04
A_23_P43484	NM_058197	<i>CDKN2A</i>	Cyclin-dependent kinase inhibitor 2A (melanoma, p16, inhibits CDK4)	2.52	1.26E-04
A_32_P28704	N/A	N/A		2.52	1.26E-04
A_24_P351466	NM_020890	<i>KIAA1524</i>	KIAA1524	2.5	1.26E-04
A_24_P334248	NM_014996	<i>PLCH1</i>	Phospholipase C, eta 1	2.48	1.26E-04
A_23_P88331	NM_014750	<i>DLGAP5</i>	Discs, large (<i>Drosophila</i>) homolog-associated protein 5	2.47	1.26E-04
A_32_P31021	N/A	N/A		2.46	1.26E-04
A_23_P361419	NM_018369	<i>DEPDC1B</i>	DEP domain containing 1B	2.45	1.26E-04
A_23_P397341	NM_152341	<i>PAQR4</i>	Progesterin and adipoQ receptor family member IV	2.42	1.26E-04
A_23_P140316	NM_001099652	<i>GPR137C</i>	G protein-coupled receptor 137C	2.42	1.26E-04
A_23_P217049	NM_014286	<i>FREQ</i>	Frequenin homolog (<i>Drosophila</i>)	2.41	2.33E-04
A_32_P35839	N/A	N/A		2.4	1.26E-04
A_24_P857404	NM_001093725	<i>MEX3A</i>	mex-3 homolog A (<i>C. elegans</i>)	2.4	1.26E-04
A_24_P323598	NM_001017420	<i>ESCO2</i>	Establishment of cohesion 1 homolog 2 (<i>S. cerevisiae</i>)	2.36	1.26E-04
A_23_P112673	NM_017975	<i>ZWILCH</i>	Zwilch, kinetochore associated, homolog (<i>Drosophila</i>)	2.33	1.26E-04
A_24_P296254	NM_014783	<i>ARHGAP11A</i>	Rho GTPase activating protein 11A	2.32	1.26E-04

N/A, not annotated; P-value, Benjamini-Hochberg false discovery rate of random permutation test; log fold change, between groups. Gene symbol, accession number and gene name were exported from GeneSpring (from the NCBI databases).

sub-G1 population (siEGFP:siASPM, 9.86:43.68%) at 6 days (Fig. 5A). On the other hand, reduced *CENPK* expression resulted in an increase in the proportion of G0/G1 phase cells (siEGFP:siCENPK, 56.49:72.2%) in MDA-MB-231 after 2 days of transfection, and a subsequent increase in the sub-G1 population (siEGFP:siCENPK, 12.73:30.96%) at 6 days (Fig. 5B). Interestingly, we observed an enlarged size of HCC1937 cells, which was likely due to abnormal tubulin formation due to decreased *ASPM* expression (Fig. 5C, arrowheads). In addition, we observed a disruption in the structural integrity of tubulin in *CENPK*-depleted MDA-MB-231 cells (Fig. 5D, arrowheads), compared with those in siEGFP-transfected cells.

These results suggest that the absence of *ASPM* and *CENPK* caused an arrest in the G2/M and G0/G1 phases, respectively,

and then induced cell death. Taken together, these findings strongly suggest that *ASPM* and *CENPK* have indispensable roles in cell proliferation and mitosis, especially in the G2/M and G0/G1 phases, in TNBC cells.

Discussion

TNBC patients do not benefit from endocrine therapy and trastuzumab. Conventional chemotherapy is currently the mainstay of systemic medical treatment, although TNBC patients have a worse outcome after chemotherapy than patients with other breast subtypes. In particular, because cytotoxic drugs often cause severe adverse effects, it is obvious that thoughtful selection of novel target molecules based on the detailed molecular mechanisms of TNBC carcinogenesis

Table V. Genes listed in cluster 1 and cluster 2.

No. of genes	Genes
Cluster 1 (enrichment score, 29.90) 87	<i>BLM, CKS1B, CKS2, CHEK1, E2F1, E2F2, E2F8, FANCA, FANCI, H2AFX, HORMAD1, HJURP, MAD2L1, NDC80, NEK2, NUF2, OIP5, PBK, RAD51, RAD54L, SPC25, TPX2, TTK, ZWINT, ZWILCH, ANLN, ASPM, AURKA, BIRC5, BUB1, BUB1B, CASC5, CDC25A, CDC6, CDCA2, CDCA5, CDCA8, CENPA, CENPF, CEP55, CHAF1B, SKA3, C13orf34, CIT, CLSPN, CCNA2, CCNB1, CCNE1, CCNE2, CDKN2A, CDKN2C, CDKN3, DSCC1, DLGAP5, ESCO2, EXO1, FAM83D, GSG2, INHBA, KIF11, KIF14, KIF18A, KIF18B, KIF20A, KIF23, KIF2C, KIFC1, LMNB1, MND1, NCAPG, NUSAP1, PTTG1, PLK1, PLK4, PKMYT1, PRC1, RBL1, SGOL2, SPAG5, STMN1, SMC4, TMSB15A, TOP2A, TACC3, TUBB3, UBE2C, UHRF1</i>
Cluster 2 (enrichment score, 6.43) 45	<i>ADAMTS5, MAMDC2, SPARCL1, WIF1, AZGP1, APOD, FIGF, CHL1, CCL28, CXCL2, COL4A6, COL14A1, COL17A1, CNTNAP3, DKK3, DST, FGF1, FMOD, HS3ST4, IGJ, IL33, LAMA3, LAMAB, LTBP2, LIFR, LRP2, MASP2, MATN2, MGP, NTN4, NRG1, PTHLH, P115, PLAT, PDGFA, PTN, PIGR, PIP, SCGB1D1, SCGB1D2, SCGB3A1, SEMA3G, STC2, THSD4, TFF3</i>

Genes enriched in cluster 1 and cluster 2 according to DAVID.

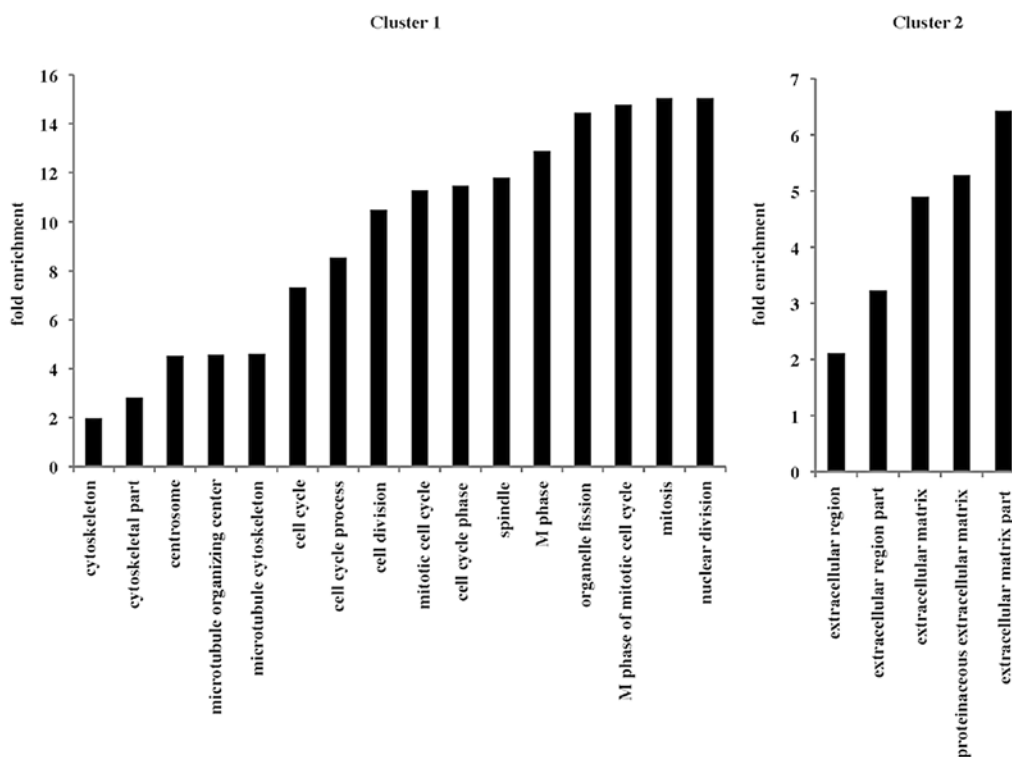


Figure 2. Gene annotation enrichment analysis based on DAVID was performed to elucidate the biological processes and pathways characterized in TNBC. Functional annotation terms are shown in bar plots; the value of the vertical axis represents the fold enrichment score of each term.

should be very helpful to develop effective anticancer drugs with a minimum risk of side effects. To this end, we performed

DNA microarray using the microdissected TNBC and normal ductal cells, and normal human vital organs including the

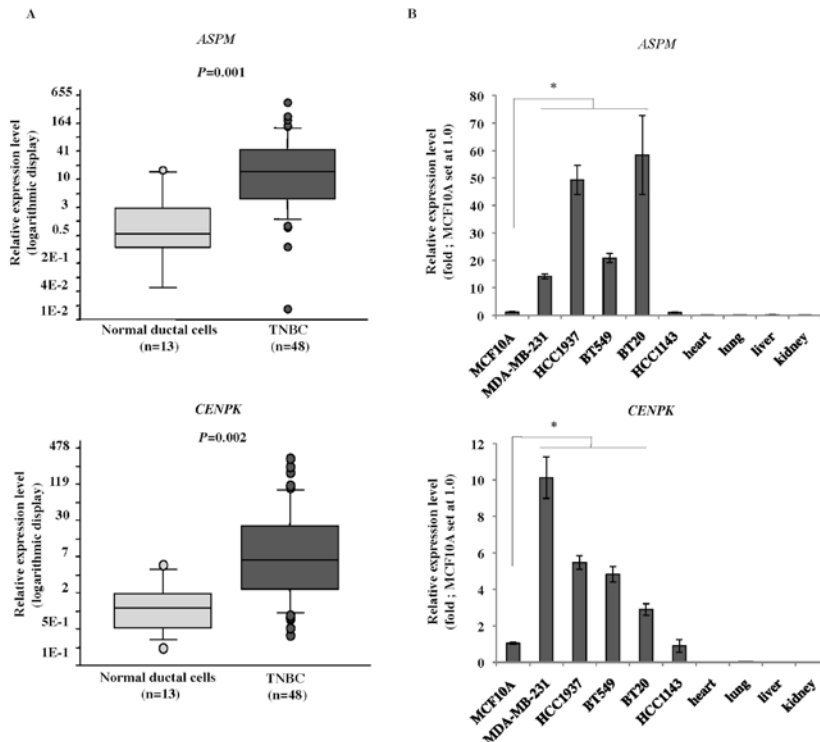


Figure 3. *ASPM* and *CENPK* expression profiles. (A) qRT-PCR results of *ASPM* and *CENPK* in microdissected tumor cells from 48 TNBC tissues and 13 normal ductal cells (Mann-Whitney t-test). (B) qRT-PCR results of *ASPM* and *CENPK* in five TNBC cell lines, MCF10A cells (human normal mammary epithelial cell line) and various normal organs (Student's two-sided t-test: * $P < 0.05$).

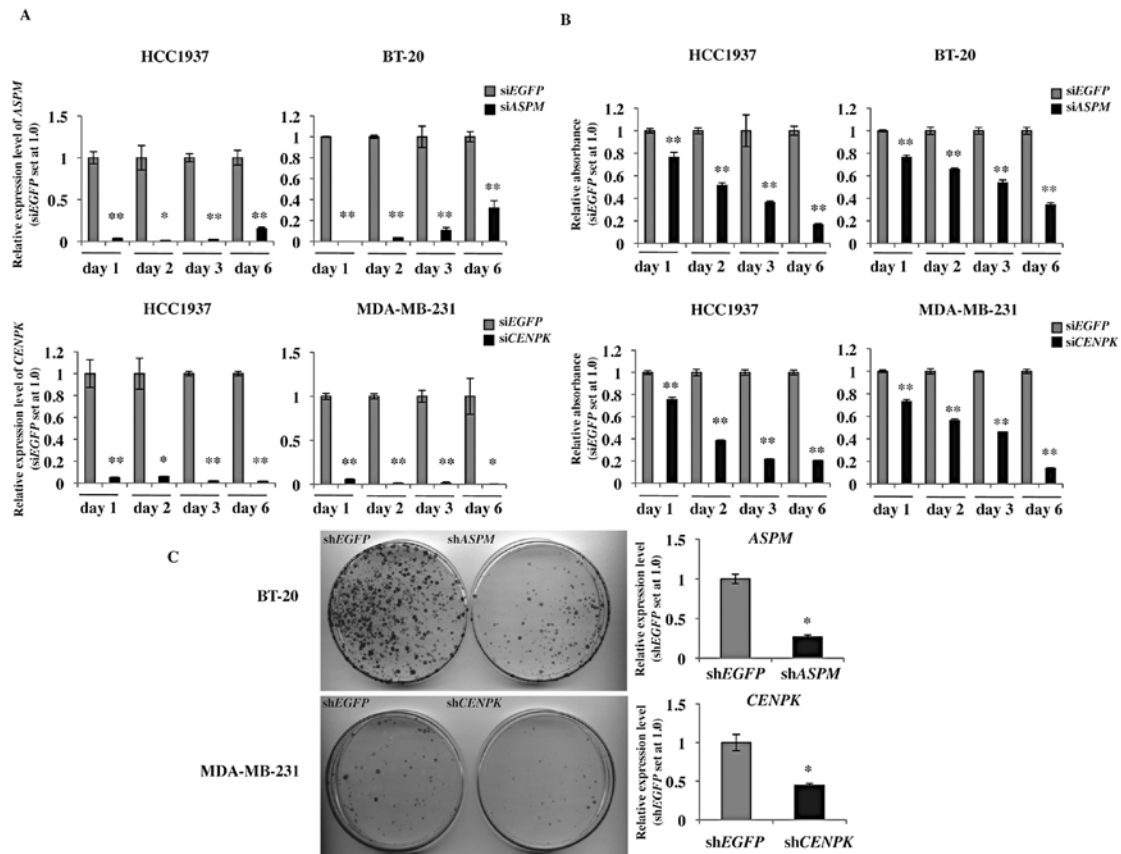


Figure 4. siRNA-mediated growth inhibitory effects in TNBC cells. (A) siRNA-mediated knockdown of *ASPM* in HCC1937 and BT-20 cells, and *CENPK* in HCC1937 and MDA-MB-231 cells was validated by qRT-PCR analysis (Student's two-sided t-test: * $P < 0.05$, ** $P < 0.01$). (B) The MTT assay showing a decrease in the number of cells upon *ASPM* knockdown in HCC1937 and BT-20 cells and *CENPK* knockdown in HCC1937 and MDA-MB-231 cells (Student's two-sided t-test: * $P < 0.05$, ** $P < 0.01$). (C) Colony formation assay (left) demonstrating a decrease in the number of colonies upon *ASPM* and *CENPK* knockdown (right) (Student's two-sided t-test: * $P < 0.05$).

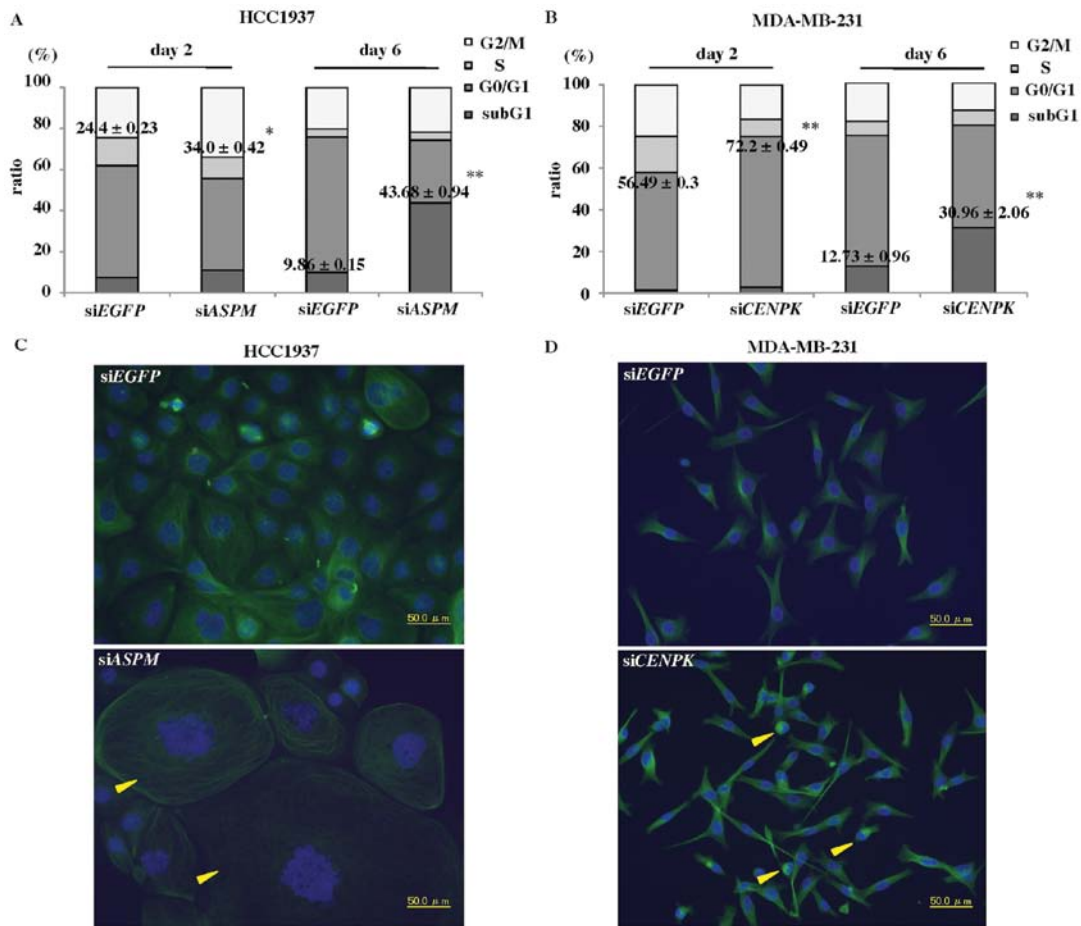


Figure 5. Alteration of the cell cycle and changes in cancer cell morphology upon *ASPM* and *CENPK* knockdown in TNBC cells. (A) FACS analysis at each time-point. The proportion of cells at the G2/M phase was elevated 2 days after si*ASPM* transfection followed by sub-G1 induction at 6 days in HCC1937 cells. (B) Upon *CENPK* knockdown, the proportion of cells at the G0/G1 phase was elevated in MDA-MB-231 cells at 2 days after si*CENPK* transfection, followed by sub-G1 induction at 6 days after transfection. A total of 10,000 cells were counted (Student's two-sided t-test: * $P < 0.05$, ** $P < 0.01$). (C) Immunocytochemical staining analysis of α/β -tubulin at 48 h after siRNA transfection. Enlarged si*ASPM*-treated HCC1937 cells (arrowhead). Control cells that entered metaphase are indicated by the arrow. (D) Disruption of the structural integrity of tubulin in si*CENPK*-treated MDA-MB-231 cells (arrowhead). α/β -tubulin and nuclei staining are shown as green and blue, respectively. Scale bars, 50 μm .

heart, lung, liver and kidney and identified 104 genes that were significantly upregulated in TNBC compared to normal duct cells, but not expressed in normal human vital organs. They included cancer specific kinases, such as *NEK2*, *PBK*, and *MELK*, which might serve as druggable targets for new therapeutic agents against TNBC.

NEK2, a member of the NIMA-related serine/threonine kinase family, is involved in cell division and the mitotic regulation by centrosome splitting, and is upregulated in a wide variety of human cancers including breast cancer (40). siRNA-mediated depletion of *NEK2* expression results in growth suppression of breast and colorectal cancers (29,30). *PBK*, a mitotic serine/threonine kinase, is significantly upregulated in the majority of breast cancers. siRNA-mediated knockdown of *PBK* expression also results in significant suppression of cell growth due to cytokinetic failure (31). *MELK*, a member of the snf1/AMPK serine-threonine kinase family, is involved in mammalian embryonic development and is also frequently upregulated in breast cancers and brain tumors (33,41). Suppression of *MELK* expression by siRNA significantly inhibits the growth of human breast cancer cells (33). These findings strongly suggest that

these cancer-specific kinases, *NEK2*, *PBK* and *MELK*, are promising therapeutic targets for TNBC.

Furthermore, we performed a gene-annotation enrichment analysis using DAVID based on gene expression profiling to elucidate the biological processes and pathways associated with each gene cluster. We found that the vast majority of genes upregulated in TNBC are functionally responsible for cell cycle progression involved in nuclear division, microtubule organization, kinetochore, and chromosome segregation, and that most inactivated functions closely related to TNBC progression are involved in cell-cell or cell-matrix interactions, which is consistent with epithelial mesenchymal transition (EMT) features as a phenotype of TNBC (42).

To further the development of novel anticancer drugs with minimum adverse effects, we focused on the cancer-specific cell-cycle associated genes *ASPM* and *CENPK* as novel molecular targets for TNBC therapy. *ASPM* has been reported to play an essential role in nucleating microtubules at centrosomes, to localize to the spindle poles during mitosis (39) and to contribute to glioblastoma cell growth (43), but has not been associated with breast carcinogenesis, especially

TNBC. Here, we confirmed that *ASPM* is upregulated in clinical samples and TNBC cell lines (Fig. 3) and that siRNA-mediated knockdown of endogenous *ASPM* results in the loss of nucleating microtubules through mitosis by impeding centrosome function, resulting in G2/M cell cycle arrest and subsequent apoptosis. These results suggest that aberrant *ASPM* expression might be involved in the carcinogenesis of TNBC and that *ASPM* targeting might be an attractive therapeutic option with less adverse effects. *CENPK* is known to be a subunit of the *CENPH-I* complex, and essential for proper kinetochore assembly (39), but little is known about the roles of *CENPK* in human cancer growth, progression, and carcinogenesis. We also confirmed that *CENPK* is upregulated in clinical samples and TNBC cell lines, and that siRNA-mediated knockdown also causes cell growth inhibition through G0/G1 cell cycle arrest due to a loss of correct tubulin structures (Figs. 3-5). Interestingly, we determined that other centromere or kinetochore-associated proteins, *CENPA*, *CENPF*, *CENPI*, *CENPM*, *NDC80* and *HJURP*, were also significantly overexpressed in TNBC cases, but not expressed in normal vital organs (Fig. 1C and Table IV). Human *CENPA* was first identified based on autoantibodies found in patients suffering from scleroderma (44) and is overexpressed in colorectal cancers (45). *CENPF* is also reportedly upregulated in head and neck squamous cell carcinomas and pancreatic ductal carcinomas (46,47). *NDC80* and *HJURP* are reportedly overexpressed in breast cancers and associated with tumor grade and poor prognosis (48,49). These findings suggest that aberrant regulation of kinetochore assembly and centromere function through mitosis might contribute to the carcinogenesis of TNBC and that destroying one component of the kinetochore, such as targeting *CENPK*, might be a novel molecular target for TNBC treatment.

TNBC is a heterogeneous subgroup of breast cancers; therefore oncologists, pathologists, and geneticists had tried to clarify TNBC by means of gene expression profiling and immunohistochemical analyses. We also applied unsupervised 2-dimensional hierarchical clustering analysis to groups of genes based on similarities in the expression pattern, but there is no clustering for TNBC based on gene expression patterns, probably due to the small sample size (data not shown). However, the information provided in this study will facilitate the development of novel and attractive molecular drug targets without adverse events.

Acknowledgements

We thank Dr Tomoya Fukawa and Dr Le Tan Dat for helpful and constructive discussions and Ms. Hitomi Kawakami for technical assistance in microdissection. This work was supported in part by a grant from Health Labour Research Grant 'Third Term Comprehensive Control Research for Cancer (H24-3rd-Gan-Ippan-006)', and Kobayashi Foundation for cancer Research (2009) (TK).

References

- Jemal A, Siegel R, Ward E, Hao Y, Xu J, Murray T and Thun MJ: Cancer Statistics, 2008. *CA Cancer J Clin* 58: 71-96, 2008.
- Di Cosimo S and Baselga J: Management breast cancer with targeted agents: importance of heterogeneity. *Nat Rev Clin Oncol* 7: 139-147, 2010.
- Rahman M, Pumphrey JG and Lipkowitz S: The TRAIL to targeted therapy of breast cancer. *Adv Cancer Res* 103: 43-73, 2009.
- Smith I, Procter M, Gelber RD, Guillaume S, Feyereislova A, Dowsett M, Goldhirsch A, Untch M, Mariani G, Baselga J, Kaufmann M, Cameron D, Bell R, Bergh J, Coleman R, Wardley A, Harbeck N, Lopezs RI, Mallmann P, Gelmon K, Wilcken N, Wist E, Sánchez Rovira P and Piccart-Gebhart MJ: HERA study team: 2-year follow-up of trastuzumab after adjuvant chemotherapy in HER2-positive breast cancer: a randomised controlled trial. *Lancet* 369: 29-36, 2007.
- Romond EH, Perez EA, Bryant J, Suman VJ, Geyer CE Jr, Davidson NE, Tan-Chiu E, Martino S, Paik S, Kaufman PA, Swain SM, Pisansky TM, Fehrenbacher L, Kutteh LA, Vogel L, Visscher DW, Yothers K, Jenkins RB, Brown AM, Dakhil SR, Mamounas EP, Lingle WL, Klein PM, Ingle JN and Wolmark N: Trastuzumab plus adjuvant chemotherapy for operable HER2-positive breast cancer. *N Engl J Med* 353: 1673-1684, 2005.
- Joensuu H, Kellokumpu-Lehtinen PL, Bono P, Alanko T, Kataja V, Asola R, Utriainen T, Kokko R, Hemminki A, Tarkkanen M, Turpeenniemi-Hujanen T, Jyrkkio S, Flander M, Helle L, Ingalsuo S, Johansson K, Jaaskelainen AS, Pajunen M, Rauhala M, Kaleva-Kerola J, Salminen T, Leinonen M, Elomaa I and Isola J, for the FinHer Study Investigators: Adjuvant docetaxel or vinorelbine with or without trastuzumab for breast cancer. *N Engl J Med* 354: 809-820, 2006.
- Foulkes WD, Smith IE and Reis-Filho JS: Triple-negative breast cancer. *N Engl J Med* 363: 1938-1948, 2010.
- Liedtke C, Mazouni C, Hess KR, André F, Tordai A, Mejia JA, Symmans WF, Gonzalez-Angulo AM, Hennessy B, Green M, Cristofanilli M, Hortobagyi GN and Pusztai L: Response to neoadjuvant therapy and long-term survival in patients with triple-negative breast cancer. *J Clin Oncol* 26: 1275-1281, 2008.
- Petricoin EF III, Hackett JL, Lesko LJ, Puri RK, Gutman SI, Chumakov K, Woodcock J, Feigal DW Jr, Zoon KC and Sistiare FD: Medical applications of microarray technologies: a regulatory science perspective. *Nat Genet* 32: 474-479, 2002.
- Huang DW, Sherman BT and Lempicki RA: Systematic and integrative analysis of large gene lists using DAVID Bioinformatics Resources. *Nat Protoc* 4: 44-57, 2009.
- Huang DW, Sherman BT and Lempicki RA: Bioinformatics enrichment tools: paths toward the comprehensive functional analysis of large gene lists. *Nucleic Acids Res* 37: 1-13, 2009.
- Hao JM, Chen JZ, Sui HM, Si-Ma XQ, Li GQ, Liu C, Li JL, Ding YQ and Li JM: A five-gene signature as a potential predictor of metastasis and survival in colorectal cancer. *J Pathol* 220: 475-489, 2010.
- Ueki T, Park JH, Nishidate T, Kijima K, Hirata K, Nakamura Y and Katagiri T: Ubiquitination and downregulation of BRCA1 by ubiquitin-conjugating enzyme E2T overexpression in human breast cancer cells. *Cancer Res* 69: 8752-8760, 2009.
- Loussouarn D, Campion L, Leclair F, Campone M, Charbonnel C, Ricolleau G, Gouraud W, Bataille R and Jézéquel P: Validation of UBE2C protein as a prognostic marker in node-positive breast cancer. *Br J Cancer* 101: 166-173, 2009.
- Arumugam T and Logsdon CD: S100P: a novel therapeutic target for cancer. *Amino Acids* 41: 893-899, 2011.
- Xiang T, Li L, Yin X, Yuan C, Tan C, Su X, Xiong L, Putti TC, Oberst M, Kelly K, Ren G and Tao Q: The ubiquitin peptidase UCHL1 induces G0/G1 cell cycle arrest and apoptosis through stabilizing p53 and is frequently silenced in breast cancer. *PLoS One* 7: e29783, 2012.
- Yoon CH, Kim MJ, Lee H, Kim RK, Lim EJ, Yoo KC, Lee GH, Cui YH, Oh YS, Gye MC, Lee YY, Park IC, An S, Hwang SG, Park MJ, Suh Y and Lee SJ: PTTG1 oncogene promotes tumor malignancy via epithelial to mesenchymal transition and expansion of cancer stem cell population. *J Biol Chem* 287: 19516-19527, 2012.
- Jin W, Liu Y, Xu SG, Yin WJ, Li JJ, Yang JM and Shao ZM: UHRF1 inhibits MDR1 gene transcription and sensitizes breast cancer cells to anticancer drugs. *Breast Cancer Res Treat* 124: 39-48, 2010.
- Ford HL, Landesman-Bollag E, Dacwag CS, Stukenberg PT, Pardee AB and Seldin DC: Cell cycle-regulated phosphorylation of the human SIX1 homeodomain protein. *J Biol Chem* 275: 22245-22254, 2000.

20. Shimo A, Nishidate T, Ohta T, Fukuda M, Nakamura Y and Katagiri T: Elevated expression of protein regulator of cyto-kinesis 1, involved in the growth of breast cancer cells. *Cancer Sci* 98: 174-181, 2007.
21. Di Leo A and Isola J: Topoisomerase II alpha as a marker predicting the efficacy of anthracyclines in breast cancer: are we at the end of the beginning? *Clin Breast Cancer* 4: 179-186, 2003.
22. Nakagawa M, Bando Y, Nagao T, Morimoto M, Takai C, Ohnishi T, Honda J, Moriya T, Izumi K, Takahashi M, Sasa M and Tangoku A: Expression of p53, Ki-67, E-cadherin, N-cadherin and TOP2A in triple-negative breast cancer. *Anticancer Res* 31: 2389-2393, 2011.
23. Adélaïde J, Finetti P, Bekhouche I, Repellini L, Geneix J, Sircoulomb F, Charafe-Jauffret E, Cervera N, Desplans J, Parzy D, Schoenmakers E, Viens P, Jacquemier J, Birnbaum D, Bertucci F and Chaffanet M: Integrated profiling of basal and luminal breast cancers. *Cancer Res* 67: 11565-11575, 2007.
24. Liu RZ, Graham K, Glubrecht DD, Germain DR, Mackey JR and Godbout R: Association of FABP5 expression with poor survival in triple-negative breast cancer: implication for retinoic acid therapy. *Am J Pathol* 178: 997-1008, 2011.
25. Kalashnikova EV, Revenko AS, Gemo AT, Andrews NP, Tepper CG, Zou JX, Cardiff RD, Borowsky AD and Chen HW: ANCCA/ATAD2 overexpression identifies breast cancer patients with poor prognosis, acting to drive proliferation and survival of triple-negative cells through control of B-Myb and EZH2. *Cancer Res* 70: 9402-9412, 2010.
26. Parris TZ, Danielsson A, Nemes S, Kovács A, Delle U, Fallenius G, Möllerström E, Karlsson P and Helou K: Clinical implications of gene dosage and gene expression patterns in diploid breast carcinoma. *Clin Cancer Res* 16: 3860-3874, 2010.
27. Ai L, Tao Q, Zhong S, Fields CR, Kim WJ, Lee MW, Cui Y, Brown KD and Robertson KD: Inactivation of Wnt inhibitory factor-1 (WIF1) expression by epigenetic silencing is a common event in breast cancer. *Carcinogenesis* 27: 1341-1348, 2006.
28. Cheng CJ, Lin YC, Tsai MT, Chen CS, Hsieh MC, Chen CL and Yang RB: SCUBE2 suppresses breast tumor cell proliferation and confers a favorable prognosis in invasive breast cancer. *Cancer Res* 69: 3634-3641, 2009.
29. Tsunoda N, Kokuryo T, Oda K, Senga T, Yokoyama Y, Nagino M, Nimura Y and Hamaguchi M: Nek2 as a novel molecular target for the treatment of breast carcinoma. *Cancer Sci* 100: 111-116, 2009.
30. Suzuki K, Kokuryo T, Senga T, Yokoyama Y, Nagino M and Hamaguchi M: Novel combination treatment for colorectal cancer using Nek2 siRNA and cisplatin. *Cancer Sci* 101: 1163-1169, 2010.
31. Park JH, Lin ML, Nishidate T, Nakamura Y and Katagiri T: PDZ-binding kinase/T-LAK cell-originated protein kinase, a putative cancer/testis antigen with an oncogenic activity in breast cancer. *Cancer Res* 66: 9186-9195, 2006.
32. Ueki T, Nishidate T, Park JH, Lin ML, Shimo A, Hirata K, Nakamura Y and Katagiri T: Involvement of elevated expression of multiple cell-cycle regulator, DTL/RAMP (denticleless/RA-regulated nuclear matrix associated protein), in the growth of breast cancer cells. *Oncogene* 27: 5672-5683, 2008.
33. Lin ML, Park JH, Nishidate T, Nakamura Y and Katagiri T: Involvement of maternal embryonic leucine zipper kinase (MELK) in mammary carcinogenesis through interaction with Bcl-G, a pro-apoptotic member of the Bcl-2 family. *Breast Cancer Res* 9: R17, 2007.
34. Shimo A, Tanikawa C, Nishidate T, Lin ML, Matsuda K, Park JH, Ueki T, Ohta T, Hirata K, Fukuda M, Nakamura Y and Katagiri T: Involvement of kinesin family member 2C/mitotic centromere-associated kinesin overexpression in mammary carcinogenesis. *Cancer Sci* 99: 62-70, 2008.
35. Chan SH, Yee Ko JM, Chan KW, Chan YP, Tao Q, Hyytiäinen M, Keski-Oja J, Law S, Srivastava G, Tang J, Tsao SW, Chen H, Stanbridge EJ and Lung ML: The ECM protein LTBP-2 is a suppressor of esophageal squamous cell carcinoma tumor formation but higher tumor expression associates with poor patient outcome. *Int J Cancer* 129: 565-573, 2011.
36. Sathyanarayana UG, Maruyama R, Padar A, Suzuki M, Bondaruk J, Sagalowsky A, Minna JD, Frenkel EP, Grossman HB, Czerniak B and Gazdar AF: Molecular detection of noninvasive and invasive bladder tumor tissues and exfoliated cells by aberrant promoter methylation of laminin-5 encoding genes. *Cancer Res* 64: 1425-1430, 2004.
37. Senchenko VN, Krasnov GS, Dmitriev AA, Kudryavtseva AV, Anedchenko EA, Braga EA, Pronina IV, Kondratieva TT, Ivanov SV, Zabarovsky ER and Lerman MI: Differential expression of CHL1 gene during development of major human cancers. *PLoS One* 6: e15612, 2011.
38. do Carmo Avides M and Glover DM: Abnormal spindle protein, Asp, and the integrity of mitotic centrosomal microtubule organizing centers. *Science* 283: 1733-1735, 1999.
39. Cheeseman IM, Hori T, Fukagawa T and Desai A: KNL1 and the CENP-H/I/K complex coordinately direct kinetochore assembly in vertebrates. *Mol Biol Cell* 19: 587-594, 2008.
40. Hayward DG and Fry AM: Nek2 kinase in chromosome instability and cancer. *Cancer Lett* 237: 155-166, 2006.
41. Nakano I, Shosterman-Smith M, Saigusa K, Paucar AA, Horvath S, Shoemaker L, Watanabe M, Negro A, Bajpai R, Howes A, Lelievre V, Waschek JA, Lazareff JA, Freije WA, Liao LM, Gilbertson RJ, Cloughesy TF, Geschwind DH, Nelson SF, Mischel PS, Tersikh AV and Kornblum HI: Maternal embryonic leucine zipper kinase is a key regulator of the proliferation of malignant brain tumors, including brain tumor stem cells. *J Neurosci Res* 86: 48-60, 2008.
42. Jeong H, Ryu YJ, An J, Lee Y and Kim A: Epithelial-mesenchymal transition in breast cancer correlates with high histological grade and triple-negative phenotype. *Histopathology* 60: E87-E95, 2012.
43. Horvath S, Zhang B, Carlson M, Lu KV, Zhu S, Felciano RM, Laurance MF, Zhao W, Qi S, Chen Z, Lee Y, Scheck AC, Liao LM, Wu H, Geschwind DH, Febbo PG, Kornblum HI, Cloughesy TF, Nelson SF and Mischel PS: Analysis of oncogenic signaling networks in glioblastoma identifies ASPM as a molecular target. *Proc Natl Acad Sci USA* 103: 17402-17407, 2006.
44. Moroi Y, Peebles C, Fritzler MJ, Steigerwald J and Tan EM: Autoantibody to centromere (kinetochore) in scleroderma sera. *Proc Natl Acad Sci USA* 77: 1627-1631, 1980.
45. Tomonaga T, Matsushita K, Yamaguchi S, Oohashi T, Shimada H, Ochiai T, Yoda K and Nomura F: Overexpression and mistargeting of centromere protein-A in human primary colorectal cancer. *Cancer Res* 63: 3511-3516, 2003.
46. de la Guardia C, Casiano CA, Trinidad-Pinedo J and Báez A: CENP-F gene amplification and overexpression in head and neck squamous cell carcinomas. *Head Neck* 23: 104-112, 2001.
47. Grützmann R, Pilarsky C, Ammerpohl O, Lüttges J, Böhme A, Sipsos B, Foerder M, Alldinger I, Jahnke B, Schackert HK, Kalthoff H, Kremer B, Klöppel G and Saeger HD: Gene expression profiling of microdissected pancreatic ductal carcinomas using high-density DNA microarrays. *Neoplasia* 6: 611-622, 2004.
48. Bièche I, Vacher S, Lallemand F, Tozlu-Kara S, Bennani H, Beuzelin M, Driouch K, Rouleau E, Lerebours F, Ripoche H, Cizeron-Clairac G, Spyrtos F and Lidereau R: Expression analysis of mitotic spindle checkpoint genes in breast carcinoma: role of NDC80/HEC1 in early breast tumorigenicity, and a two-gene signature for aneuploidy. *Mol Cancer* 10: 23, 2011.
49. Hu Z, Huang G, Sadanandam A, Gu S, Lenburg ME, Pai M, Bayani N, Blakely EA, Gray JW and Mao JH: The expression level of HJURP has an independent prognostic impact and predicts the sensitivity to radiotherapy in breast cancer. *Breast Cancer Res* 12: R18, 2010.